

## **Final Report**

# **Establishing the geomorphic context for wetland and riverine restoration of the San Rafael River**

**NRCS Cooperative Agreement #68-3A75-4-155**

**Stephen T. Fortney, John C. Schmidt, and David J. Dean**  
Intermountain Center for River Rehabilitation and Restoration  
Department of Watershed Sciences  
Utah State University  
Logan, UT

In collaboration with  
Michael E. Scott  
Julian Scott  
Fort Collins Science Center  
U. S. Geological Survey  
Fort Collins, CO

**March 22, 2011**

## Table of Contents

I. Introduction	5
II. Purpose	5
III. Study Area	9
IV. Hydrology	11
V. Methods	18
A. Floodplain Stratigraphy	18
B. Repeat Photography: Aerial Imagery and Oblique Ground Photographs	19
C. USGS gage data	21
Reconstructed Cross Sections	21
Rating Relations	22
Time Series of Thalweg Elevation	22
Time Series of Width and Width-to-Depth Ratio	22
Hydraulic Geometry	22
D. Longitudinal Profile	24
E. Additional Activities	24
VI. Results: Channel Transformation on Hatt Ranch	26
Turn of the 20 <sup>th</sup> century	26
1930s and 1940s	29
1950s	33
1960s and 1970s	41
1980s	46
1990s to present	49
Longitudinal Profile	50
VII. Summary	54
A. Channel Transformation on Hatt Ranch	54
B. Restoration and Management Implications	55
VIII. Expenditures	56
IX. Timeline	56
X. References	56
XI. Appendix	59

## Table of Figures

Figure 1. Oblique ground photos taken near the old Highway 24 bridge	6
Figure 2. Conceptual model of how watershed attributes control channel and floodplain form.	7
Figure 3. Conceptual model of restoration versus rehabilitation	8
Figure 4. Map of the San Rafael River watershed.	10
Figure 5. Map of the study area	11
Figure 6. Characteristics of notable snowmelt floods.	15
Figure 7. Annual Peak Discharge vs. Mean Annual discharge	15
Figure 8. Median annual hydrographs for two selected time periods	16
Figure 9. Flood frequency analysis	17

Figure 10. Hydrograph for period of record	17
Figure 11. Floodplain trenches at Frenchman’s Ranch	19
Figure 12. Various locations of the USGS gage and associated cableways	25
Figure 13. Thalweg elevation time series for 1909 and 1920	27
Figure 14. Time series of width and width-to-depth ratio for entire period of record	28
Figure 15. Results from plan form analysis	30
Figure 16. Oblique ground photo omparison at the old Highway 24 bridge	31
Figure 17. Comparison of aerial photographs for a short reach downstream of the Hatt Ranch.	32
Figure 18. Thalweg elevation time series for 1947 and 1976	33
Figure 19. 1952 aerial photo of vicinity of Hatt Ranch	36
Figure 20. Cross sections and thalweg elevation time series for snowmelt flood of 1952	37
Figure 21. Reconstructed cross sections	38
Figure 22. Rating relations constructed for the time period between 1947 and 1976	38
Figure 23. Hatt Ranch floodplain stratigraphy	39
Figure 24. Series of aerial photographs shows Hatt Ranch trench	40
Figure 25. Hydraulic geometry relationships	45
Figure 26. Rating relations constructed for the time period between 1976 and 2008	48
Figure 27. Thalweg elevation time series for 1976 and 2008.	48
Figure 28. Longitudinal profile entire length of the lower San Rafael River	52
Figure 29. Longitudinal profile for a 2.25 kilometer reach upstream of Frenchman’s Ranch	53
Figure 30. Longitudinal profile for the lowest 2.25 kilometer reach of the San Rafael River	53
Figure 31. Hydrograph of the mean daily discharge for the period of record	55
Figure 32. Cross sections and thalweg elevation time series for snowmelt flood of 1949	59
Figure 33. Cross sections and thalweg elevation time series for snowmelt flood of 1957	60
Figure 34. Cross sections and thalweg elevation time series for snowmelt flood of 1958	61
Figure 35. Cross sections and thalweg elevation time series for snowmelt flood of 1962	62
Figure 36. Cross sections and thalweg elevation time series for snowmelt flood of 1965	63
Figure 37. Cross sections measured during the snowmelt floods of 1952, 1958, 1962, 1965.	64
Figure 38. Median annual hydrograph for 1910-1918 and 1945-1954	65
Figure 39. Median annual hydrograph for 1946-1954 and 1955-1963	65

## **Table of Tables**

Table 1. Mean annual flow for selected time periods	14
Table 2. Characteristics for notable snowmelt floods	14
Table 3. Statistics for each time period of adjustment shown in the MINSBE analysis	27
Table 4. Statistics for six time periods of adjustment shown in the width time series	28
Table 5. Statistics for four periods of adjustment periods in the width-to-depth ratio	28
Table 7. Plan form results	30
Table 8. Relevant information for aerial photographs analyzed in this study	40
Table 9. Width hydraulic geometry relationship formula	46
Table 10. Velocity hydraulic geometry relationship formula	46
Table 11. Depth hydraulic geometry relationship	46
Table 12. ANCOVA results for paired time periods	46
Table 13. Water surface slopes	51
Table 14. USU final invoice	56
Table 15. Timeline of remaining activities to be completed	56

## **I. Introduction**

This report summarizes research activities funded under Natural Resources Conservation Service (NRCS) Cooperative Agreement #68-3A75-4-155, “Establishing the geomorphic context for wetland and riverine restoration of the San Rafael River, UT to evaluate the effects of large-scale tamarisk (*Tamarix ramosissima*) removal on stream and riparian habitats.” Although this agreement began on January 1, 2009, significant work did not begin until spring 2009, and the first floodplain excavations were begun under the supervision of Dean Fortney began significant work on this project in summer 2009. The cooperative agreement officially ended on December 31, 2011, however research activities related to this cooperative agreement will continue through summer 2011 with supplemental funding provided by the Intermountain Center for River Rehabilitation and Restoration.

The purpose of this report is to describe all research work conducted through the end of 2010. The findings described here will be integrated with subsequent work conducted in 2011 and ultimately be reported as Fortney’s master’s thesis and as a final report to be submitted to the NRCS and other agencies involved in planning rehabilitation of the San Rafael River. Analyses presented in this report provide a description of the history of channel change throughout the twentieth century that is based on (1) interpretation of floodplain deposits exposed in one trench located on the Hatt Ranch, (2) analyses of historical aerial photography, and (3) interpretation of U. S. Geological Survey (USGS) stream-flow gage data, including cross-section measurements, hydraulic geometry, and the temporal history of changes in width and thalweg elevation. This report also describes a longitudinal profile survey of bed elevation and water surface elevation conducted for the entire lower San Rafael River. This report also provides a list of expenditures through December 31, 2010.

Subsequent analyses to be completed in 2011 include analysis of two additional trenches and analysis of other aerial photographs that allow further description of the history of channel narrowing and floodplain evolution. Future data collection will involve bed material sampling and mapping of the alluvial valley.

## **II. Purpose**

As depicted in an old photograph (Figure 1), the San Rafael River was once a wide, laterally unstable, multi-thread channel whose active bed was comprised of numerous bars. Under these geomorphic conditions, connectivity between the main stem and the floodplain presumably provided endemic fish access to food resources and diverse habitat conditions. In contrast, the current river is confined by steep, vegetated, cohesive banks and has a low width-to-depth ratio. Today, the river contains few bars and riffles, and floods rarely connect the channel with the floodplain. Despite this decrease in quality and quantity of habitat, the flannelmouth sucker

(*Catostomus Latipinnis*), bluehead sucker (*Catostomus discolor*), and roundtail chub (*Gila robusta robusta*) are still found in isolated patches of complex, heterogeneous habitat in the lower San Rafael River (Budy et al, 2010).

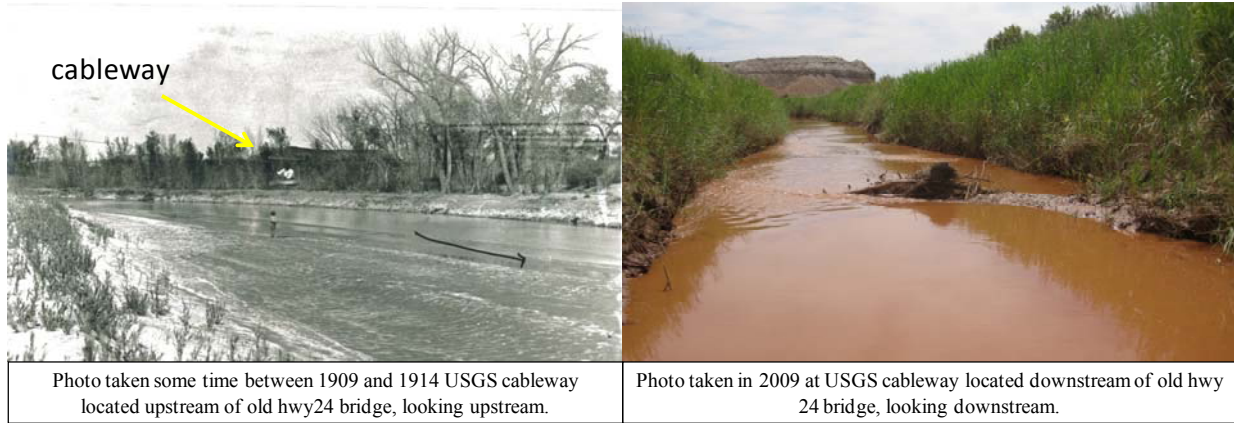


**Figure 1. Photographs of the San Rafael River in vicinity of the old Highway 24 bridge on Hatt Ranch depicting typical channel conditions (A) in the early twentieth century and (B) today.**

This study is one part of a suite of scientific studies whose goal is development of a plan for rehabilitation of the San Rafael River, especially as it pertains to rehabilitating desirable habitat for native fish species. Aquatic habitat results from the interaction of species with the river's hydraulics and geomorphic structure. Thus, the geomorphic structure of the channel – its cross-section characteristics, bed material, planform, and gradient – are a critical determinant of the habitat available to the desired species of the river (Figure 2). In turn, the geomorphic structure of a channel and its adjacent floodplain are primarily determined by the flood flows that occur in the watershed and by the amount and sizes of the sediment weathered from the bedrock of the watershed and available to be transported by the stream flow. Thus, channels may be relatively wide and shallow or narrow and deep. Channels may have sand beds or gravel beds and may, or may not, be organized into a sequence of pools and riffles. Channels may have only a single sinuous thread, or they may have many threads in which part of the total stream flow occurs. Channels may be steep or flat in gradient. The wide array of possible channel forms is generally linked to the magnitude and variability of the floods generated in the watershed and by the dominate sizes of sediment transported by those flows.

**The conceptual model that underlies fluvial geomorphology**

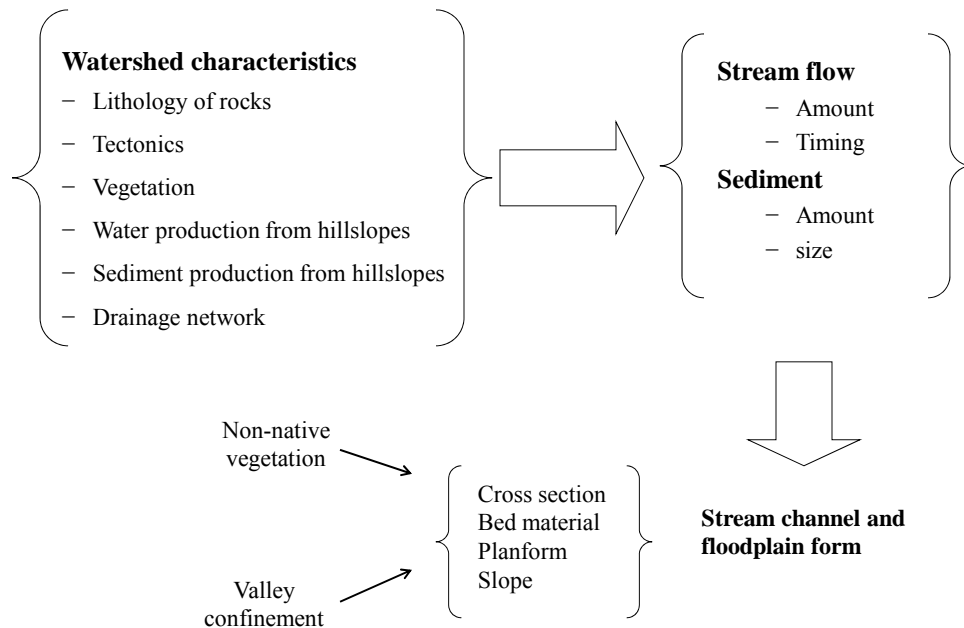


**Figure 2. Conceptual model of how watershed attributes control channel and floodplain form. There are four primary attributes of channel form, and these are primarily determined by the flux of water and by the typical sediment transported through the channel network.**

As demonstrated in this report, the geomorphic structure of the lower San Rafael River downstream from the San Rafael Reef has changed greatly during the twentieth century. These changes have occurred, because the magnitude of floods has greatly decreased while the amount of sediment available to be transported has probably changed little. The primary objective of this report is to describe the timing and magnitude of channel change. These results can be linked with a historical understanding of changes in the native fish community in order to clarify which changes in habitat had the greatest impact on the declining populations of native fish in the lower San Rafael River.

Restoration of extensively developed watersheds is impossible. In the case of the San Rafael River, there has been a significant investment in Wasatch Plateau reservoirs and in diversions to support agriculture and industry in Castle Valley. Thus, the decision concerning reversing undesired present conditions of the native fish species and their habitat is one of river rehabilitation – reversing, to some degree, present conditions yet not returning the river system to its pre-disturbance condition (Figure 3). Historical analyses of channel change, as is provided in this report, informs decisions about how much, and what kinds of, river rehabilitation are appropriate.

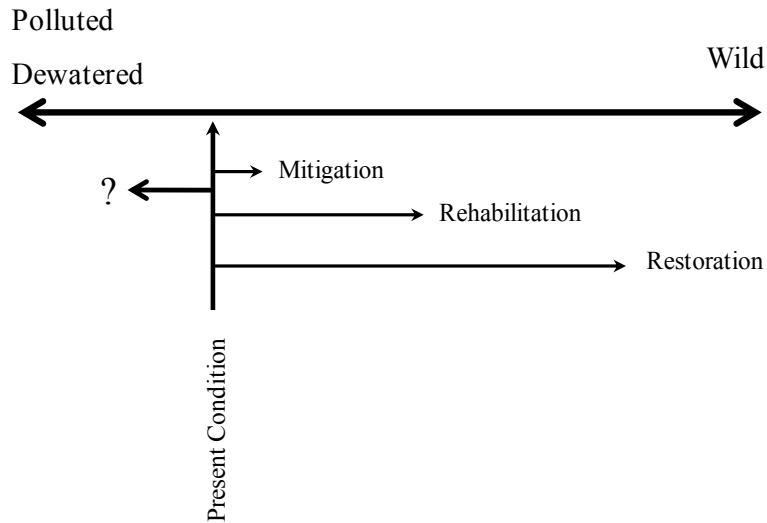


**Figure 3. Restoration is the return of an ecosystem to its pre-disturbance condition. Rehabilitation is the reestablishment of some attributes of the ecosystem to their pre-disturbance condition. In the case of the San Rafael River, complete restoration is impossible, and policy choices must be made to identify which attributes can be partly restored.**

Although the channel changes described in this report have primarily been caused by changes in stream flow, they have also been caused by invasion of the non-native shrub tamarisk (*Tamarix* spp.). Tamarisk has replaced native vegetation, especially cottonwoods and willows, in riparian corridors and wetlands in much of the southwest United States (Brock, 1994; Robinson, 1965). Friedman et al (2005) report that tamarisk is the second most abundant riparian species in the Intermountain West, today. Dense tamarisk stands increase channel roughness, which in turn slows water velocity during a flood and ultimately accelerates vertical and lateral accretion of floodplains, thereby facilitating channel narrowing (Graf, 1978, Birken and Cooper, 1980) and transforming aquatic habitat. In the San Rafael River, the invasion of tamarisk has occurred concurrently with changes to the hydrologic regime as a result of multi-decadal scale climate shifts (Hereford et al, 2002) and water development in the headwaters. This study seeks to differentiate between the influence of the altered flow regime and the influence of tamarisk establishment in causing changes in channel and floodplain form.

Efforts to restore fish habitat by removing tamarisk in the riparian corridor are currently underway along parts of the San Rafael River. However, there is no clear vision of the potential outcomes of these channel rehabilitation activities, and there is little understanding of the history of hydrologic and geomorphic change and the primary mechanisms responsible for the observed channel changes. It is the objective of this study to provide a comprehensive understanding of the rates and magnitude of channel change during the twentieth century. The results from our work will be useful in the development of a strategy for restoring the channel-floodplain connection and increasing geomorphic complexity that leads to improved fish habitat.

### **III. Study Area**

The San Rafael River drains approximately 6200 km<sup>2</sup> of east central Utah (Figure 4). The mainstem of the San Rafael River begins in Castle Valley at the junction of three streams: Huntington Creek, Cottonwood Creek, and Ferron Creek. These three streams drain the Wasatch Plateau, which is the largest of the north-south trending High Plateaus of Utah (Geary, 1996). The Wasatch Plateau, which is comprised of uplifted sedimentary rocks, is approximately 150 km long and 30 to 55 km wide. The highest elevations in the Wasatch Plateau exceed 3300 m. In an average year, the upper elevations receive approximately 1 m of precipitation, mostly in the form of snow

Castle Valley, where the San Rafael River begins, is nestled between the Wasatch Plateau and the San Rafael Swell and elevations range between 1740 m and 1920 m. Average precipitation in the valley is approximately 25 cm per year. Agriculture is the dominant land use in Castle Valley where the four largest towns in the San Rafael watershed are situated: Huntington, Castle Dale, Ferron, and Cleveland.

The San Rafael River has incised the uplifted sedimentary formations of the San Rafael Swell, an anticline approximately 160 km long and 65 km wide. On the eastern edge of the Swell is a steep monocline called the San Rafael Reef. Here, the San Rafael River exits the Swell in a dramatic fashion and begins a tortuous path across the San Rafael Desert. The San Rafael River empties into the Green River, approximately 45 km south from the town of Green River where the average annual precipitation is approximately 18 cm. The downstream 100 kilometers of the San Rafael River, which flows through the San Rafael Desert is the focus of this study (Figure 5). Here, tamarisk has colonized large swaths of the alluvial valley and changes to the cross-section geometry and plan form appear to be most pronounced.

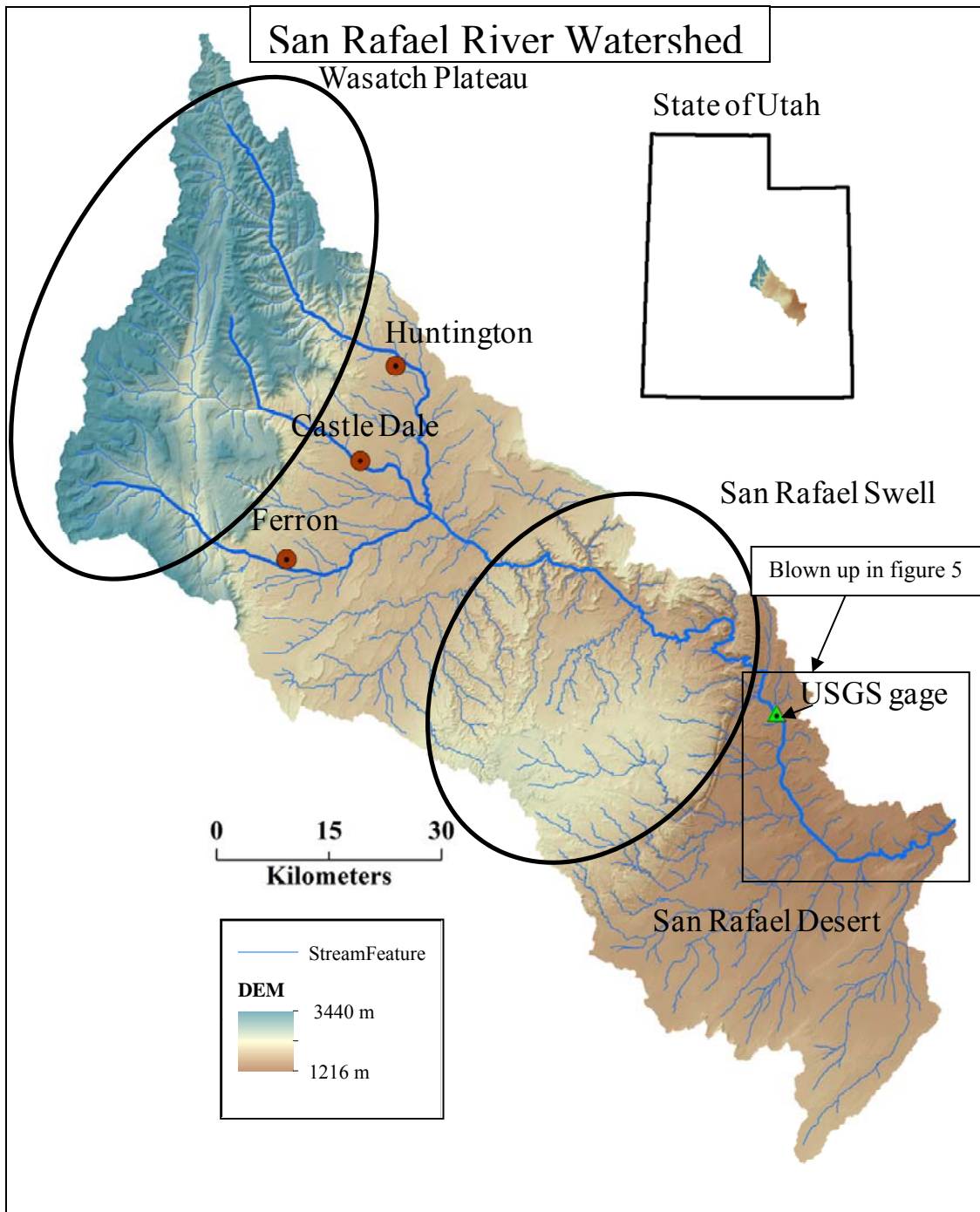


**Figure 4. Map of the San Rafael River watershed. The headwaters and the spring snowmelt flood originate in the Wasatch Plateau. Warm season precipitation events erode sedimentary formations in the San Rafael Swell and the San Rafael Desert.**

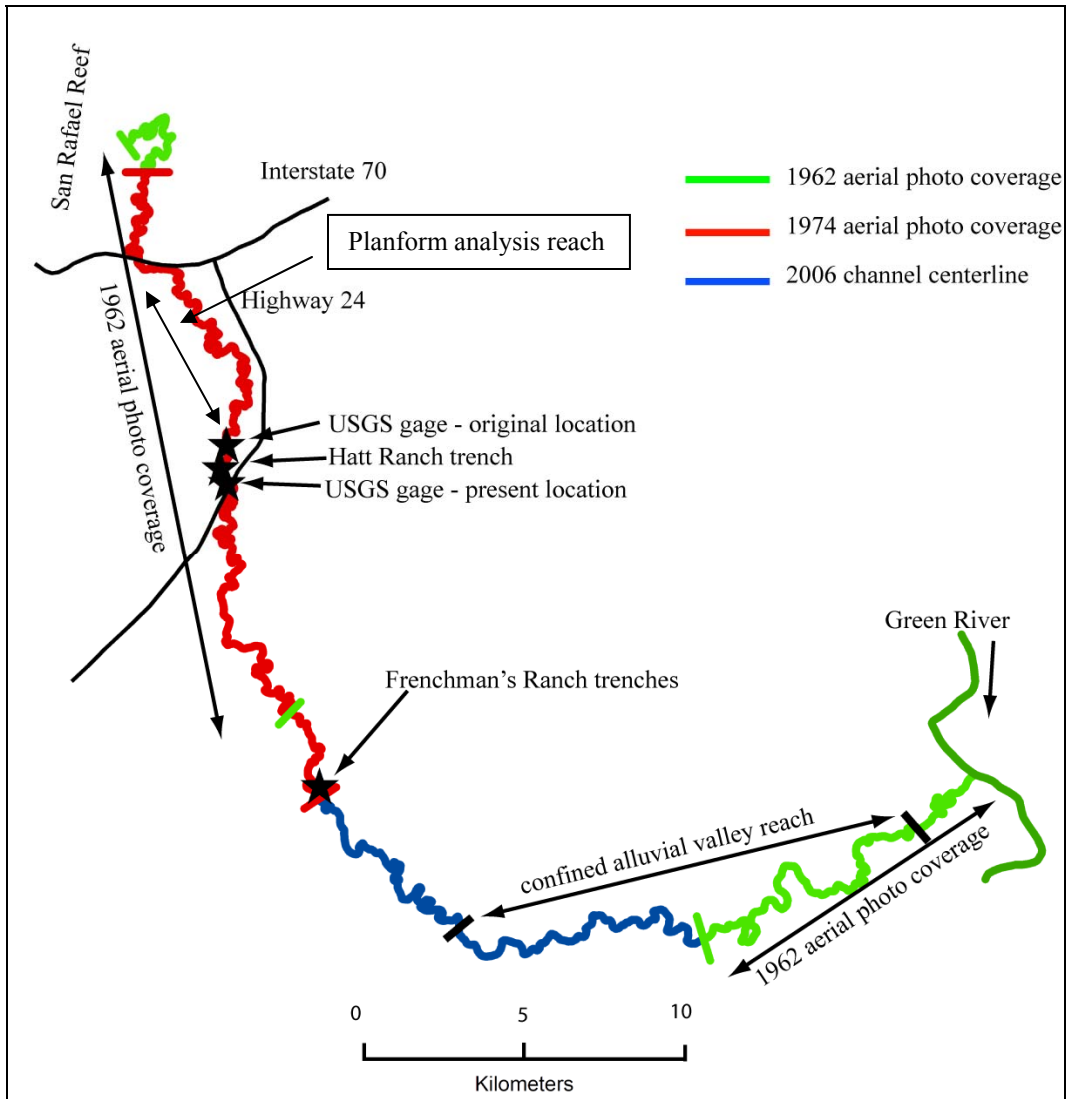


**Figure 5. Map of the study area, which extends from the San Rafael Reef to confluence with the Green River.**

#### **IV. Hydrology**

The annual hydrograph of the San Rafael River is characterized by two peaks. Snow melting on the Wasatch Plateau produces a predictable spring flood, and short duration floods in summer and fall, comprise the second type of flood peak. The North American monsoon may produce floods from intense thunderstorms during summer, and cut-off low pressure cells from dissipating tropical cyclones may produce longer duration floods in fall (Webb and Betancourt, 1990). Both types of “warm season” floods have durations between a few hours to a week. Often, the daily average discharge during the peak of a warm season flood is much less than the instantaneous peak of that flood (Figure 10). Warm season precipitation events usually occur over the downstream half of the watershed, erode the friable sedimentary formations of the San

Rafael Swell and the San Rafael Desert (figure 2), and deliver large quantities of fine sediment to the main stem channel. On the other hand, the snowmelt flood is derived from the Wasatch Plateau where there is relatively little sediment compared to the Swell, therefore the sediment transported during snowmelt floods is derived primarily from the channel banks and bed. Snowmelt floods generally last longer and are more predictable than warm season floods.

This study analyzed the hydrologic record measured at USGS gage 09328500 (San Rafael near Green River) in order to describe the typical annual hydrograph early in the twentieth century and the subsequent changes that have occurred. The gage has been in operation for 74 years. The USGS began measuring stream-flow on October 1, 1909 and halted the operation of the gage on September 30, 1918. Operation resumed 27 years later on October 1, 1945, and the USGS has continued measuring streamflow to the present.

In this study, we analyzed the stream-flow record using several metrics. We calculated median annual hydrographs for specific time periods, calculated flood frequency, and calculated duration and runoff volume for notable snowmelt floods. In order to calculate flood duration, first it was necessary to define the beginning and ending discharge of a flood. We determined the beginning of a snowmelt flood by examining the period of baseflow leading up to the flood, and then determined the day when baseflow began to steadily increase beyond the preceding month's baseflow variation. The baseflow discharge that preceded each year's flood varied greatly from year to year, and thus the baseflow discharge prior to the first day of each snowmelt flood varied. We defined the end of the flood as the return to the approximate pre-flood baseflow level. Finally, we calculated flood duration by adding all of the mean daily discharges for the chosen flood. Table 1 lists the dates chosen as the beginning and end of each flood and the discharges that occurred on those dates.

Because the snowmelt flood originates on the Wasatch Plateau where many dams have been built, the natural timing and magnitude of each year's flood has the potential to be disrupted by storage in reservoirs. Once stream flow emerges from the Plateau into Castle Valley, there are large diversions for agricultural and industrial purposes. Thus, spring snowmelt floods pass through the San Rafael Swell only when snowmelt is not stored in Wasatch Plateau reservoirs and is not diverted in Castle Valley.

In the early 20<sup>th</sup> century the median spring snowmelt flood lasted approximately 70 days and the peak was approximately 1320 ft<sup>3</sup>/s. Extensive water development, however, in conjunction with decadal scale climate shifts (Webb and Betancourt, 1992; Hereford et al 2002) drastically decreased the magnitude and duration of the annual snowmelt flood. Consequently, the median annual snowmelt flood for the period 2000-2008 lasted only 23 days, and the magnitude of the peak flow was approximately 345 ft<sup>3</sup>/s, a respective 67% and 93% reduction from the early 1900's (Figure 8). There has not been any change in the timing of the peak flow, however, the

average peak of the snowmelt flood occurred on June 4 in the early 1900s and now occurs on June 5. Since the snowmelt flood contributes a large majority of the runoff volume of the total annual yield then the decline in mean annual flow over the course of the twentieth century illustrates the decline of the snowmelt flood (Table 2). Large annual flows occurred during the period between 1980 and 1986, and temporarily interrupted the trend of declining annual stream-flow.

The largest snowmelt floods have not produced the largest peak stream-flows. For example, four out of the six years with the largest mean annual discharge (1910, 1914, 1917, 1952, 1983, 1984) were not years with especially high peak annual discharge (Figure 7). The exception is water year 1917, when both a large snowmelt flood and the second largest recorded warm season flood occurred. On the other hand, the largest peak stream-flows have occurred during warm season precipitation events, which comprise approximately two-thirds of the annual peak discharge population (Figure 7). Furthermore, large magnitude warm season events have not necessarily coincided with large snowmelt floods. For example, the years in which four of the five largest annual peak discharges occurred did not contain large snowmelt floods. Furthermore, the largest magnitude peak annual discharges and mean annual discharges, both are distinctively separate from the remaining respective populations. For example, the years in which the annual peaks were greater than 4000 ft<sup>3</sup>/s are few; only five times has this threshold been exceeded. And, the years in which the mean annual discharge exceeded 300 ft<sup>3</sup>/s occurred only six times. It should be noted that the flood of September 2, 1909, is excluded from figure 7 because no mean annual discharge is reported for this flood. Also, the color of each data point in Figure 7 is determined by the type of flood, either monsoon or snowmelt, that contained the largest instantaneous peak during the particular water year. Finally, the annual peak discharges plotted in Figure 7 are the instantaneous peak annual discharges reported on the USGS streamflow website.

The magnitude of warm season floods has also decreased. There has been a noticeable lack of large magnitude, short duration peaks since the late 1950s (Figure 10). Warm season precipitation events produced the five largest floods, all of which occurred prior to 1960 (Figure 7). In general, the removal of the snowmelt flood plus the decline in the magnitude of warm season floods has resulted in a suppressed annual hydrograph characterized by a minimal snowmelt flood and small short duration warm season events (Figure 8). Table 3 lists characteristics of notable snowmelt floods which have caused significant geomorphic change over the last century; this information will be helpful in describing the differences in snowmelt floods which have caused geomorphic changes.

**Table 1. Characteristics for notable snowmelt floods measured near Green River USGS gage**

Water Year	Duration	Runoff Volume	Begin Date	Begin Discharge	End Date	End Discharge	Peak Discharge	Date of Peak	Time to peak
	days	ac-ft		ft <sup>3</sup> /s		ft <sup>3</sup> /s	ft <sup>3</sup> /s		days
1910	120	179934	Feb-10	200	Jun-10	57	2100	May-10	73
1914	88	212151	Apr-14	156	Jul-14	115	3580	Jun-14	58
1917	105	216147	Apr-17	129	Aug-17	77	4170	Jun-17	58
1918	58	44155	May-18	170	Jul-18	152	1290	Jun-18	48
1952	104	252743	Apr-52	194	Jul-52	95	3950	Jun-52	50
1957	93	126989	May-57	70	Aug-57	82	2710	Jun-57	41
1958	86	134652	Apr-58	136	Jul-58	44	2240	May-58	43
1962	110	84005	Mar-62	74	Jul-62	58	1120	May-62	45
1965	117	145296	Apr-65	82	Aug-65	90	1940	Jun-65	66
1969	104	86421	Apr-69	110	Jul-69	88	1070	May-69	55
1970	83	69799	May-70	237	Aug-70	65	1470	Jun-70	24
1973	88	89138	Apr-73	107	Jul-73	80	1370	Jun-73	44
1980	106	104033	Apr-80	81	Aug-80	80	2040	Jun-80	52
1982	81	53927	May-82	101	Jul-82	94	880	Jun-82	49
1983	165	294220	Mar-83	169	Aug-83	100	3600	Jun-83	100
1984	153	291141	Mar-84	100	Aug-84	150	3290	Jun-84	86
1985	90	89148	Apr-85	160	Jul-85	133	1200	May-85	56
1986	122	106637	Mar-86	91	Jul-86	103	2300	Jun-86	70
1995	71	74605	May-95	60	Aug-95	74	1860	Jul-95	40
1996	80	36521	May-96	49	Jul-96	55	723	Jun-96	41
1997	54	48126	May-97	102	Jul-97	72	1170	Jun-97	30
2005	79	80095	Apr-05	45	Jul-05	39	2010	Jun-05	37
2006	99	57802	Apr-06	40	Jul-06	42	955	Jun-06	64

**Table 2. Mean annual flow for selected time periods. Time periods were chosen based on observed trends in stream-flow which also correlate to observed trends in geomorphic change**

Time Period	Mean Annual Flow (ft <sup>3</sup> /s)
1910 to 1918	272.5
1946 to 1958	144.2
1959 to 1979	92.2
1980 to 1986	255.4
1987 to 2010	67.2

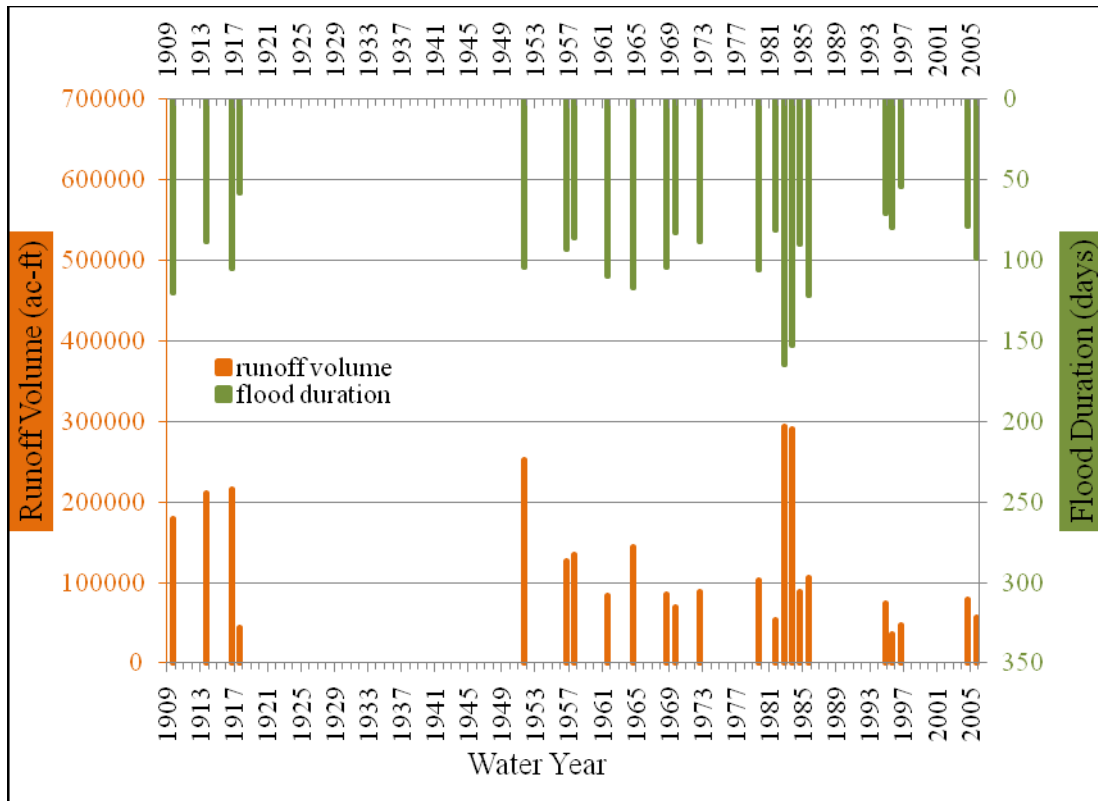


Figure 6. Two characteristics, runoff volume and flood duration, of notable snowmelt floods.

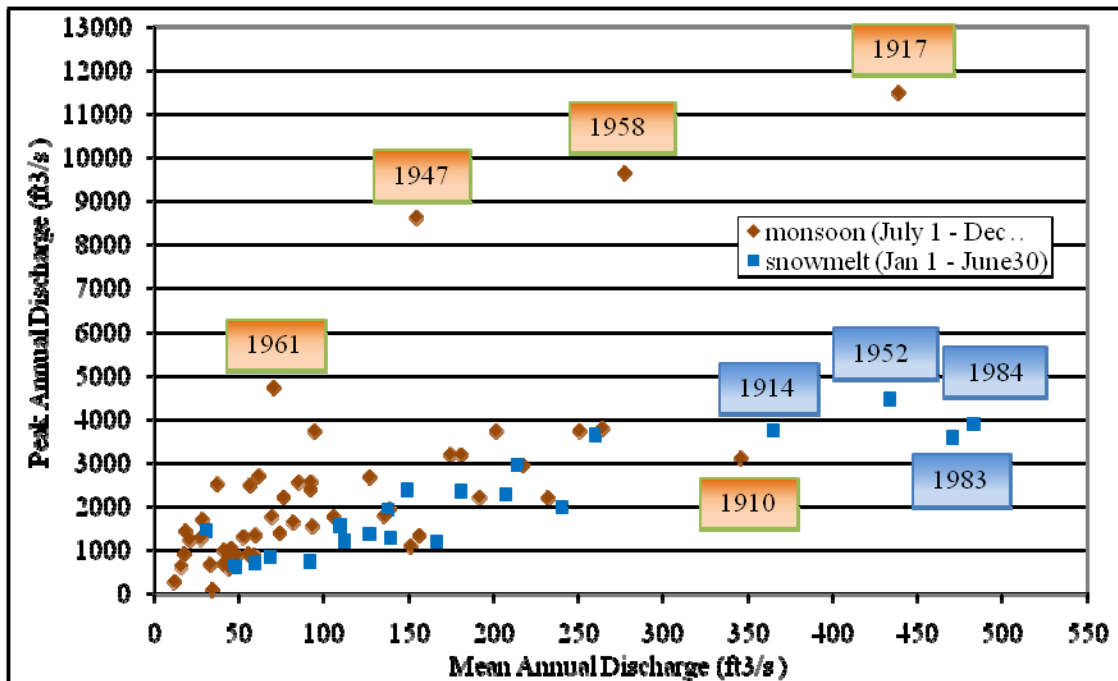


Figure 7. Annual Peak Discharge vs. Mean Annual discharge. The color of each data point is determined by the largest instantaneous peak during the particular water year. The flood of September 2, 1909, is excluded from this chart because no mean annual discharge is reported for this flood. Labels for notable data points are water years in which the peak flood occurred.

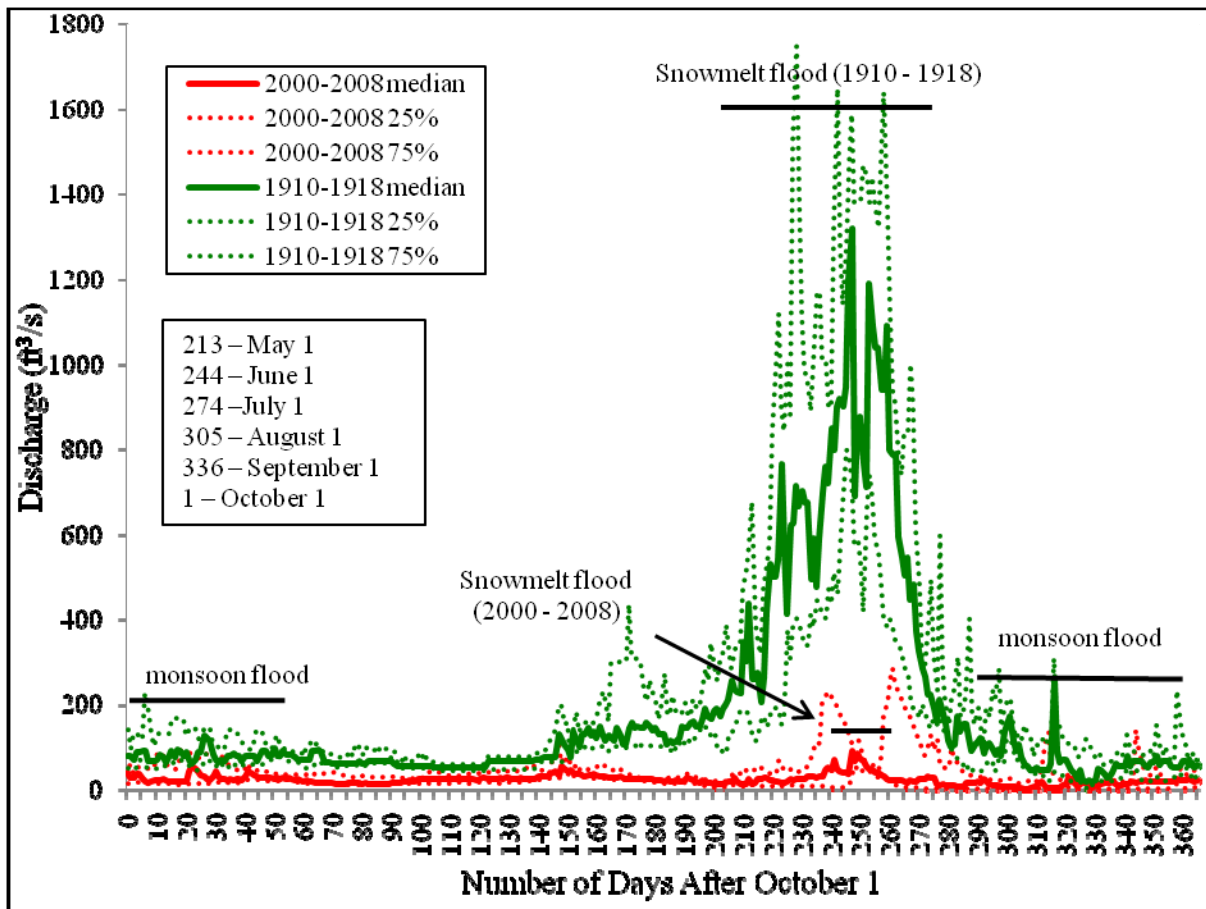


Figure 8. Median annual hydrographs for two selected time periods. Dotted lines are 75 and 25 quartiles for each time period.

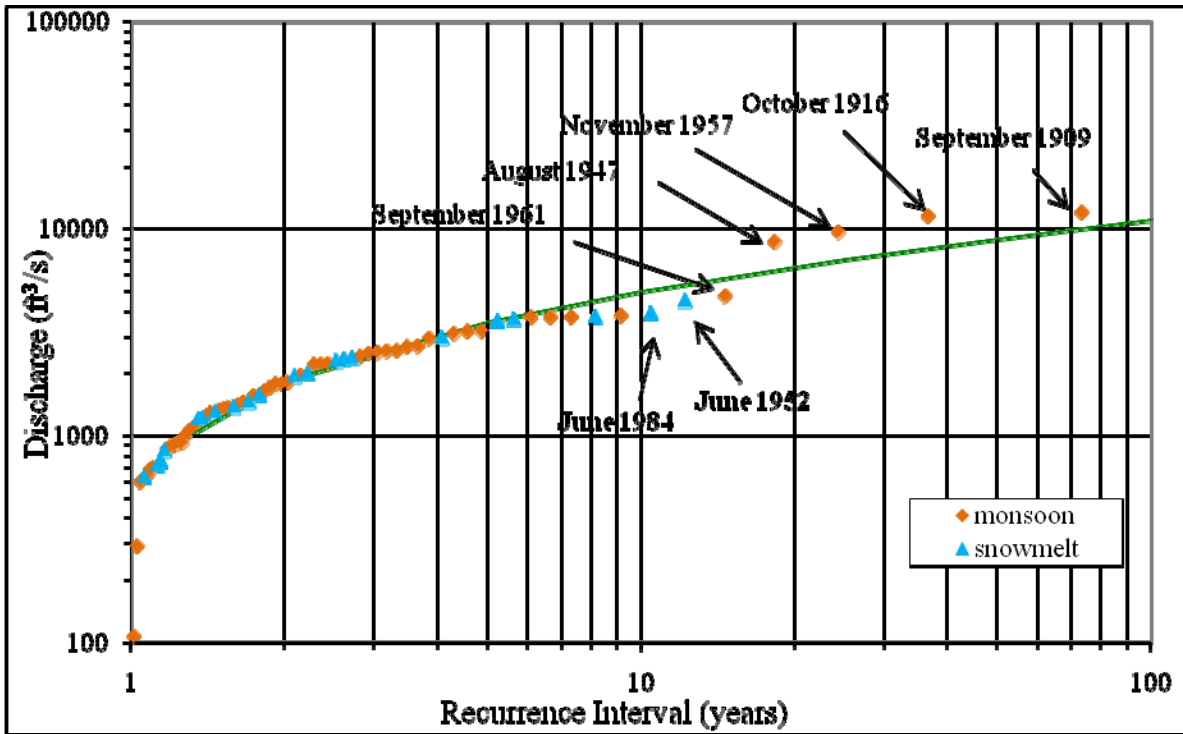


Figure 9. Flood frequency analysis of the stream flow record at the USGS gage (09328500). The instantaneous annual peak discharge data was used in this analysis. The curve represents the Log Pearson Type III fit of the plotted data.

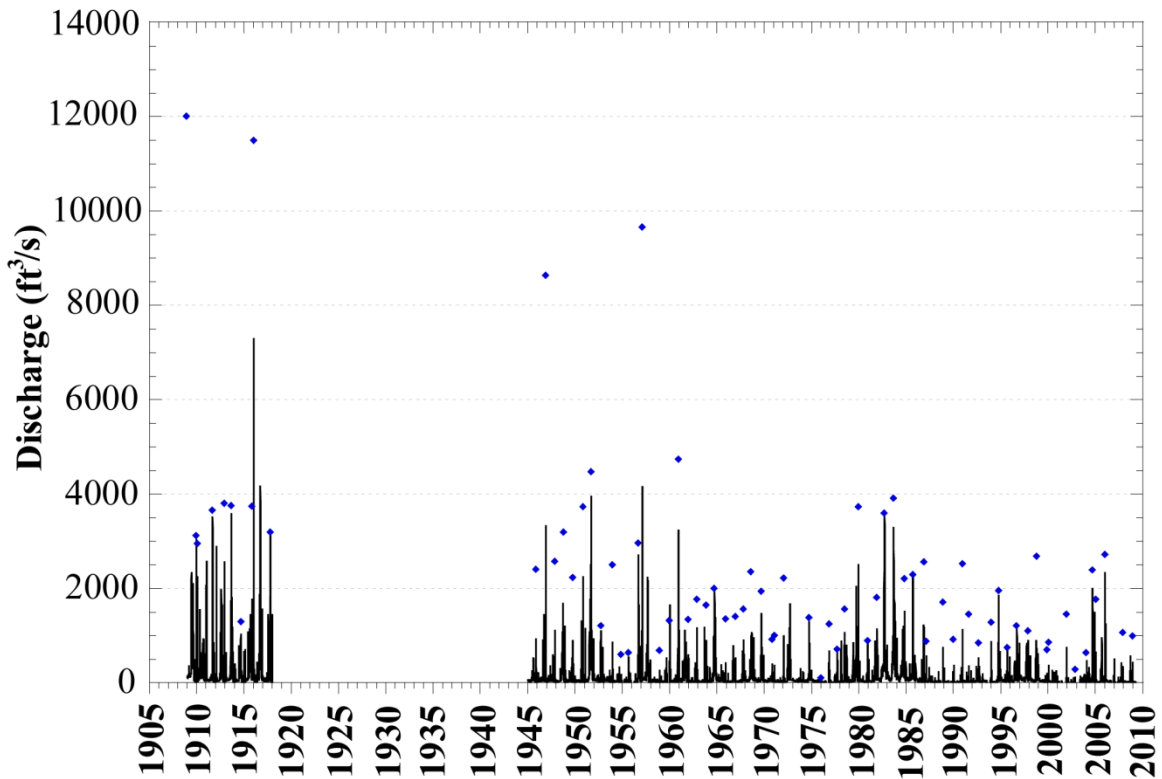


Figure 10. Time series of the mean daily discharge data shown in black, and the instantaneous peak discharge data shown as blue diamonds.

## V. Methods

This study employs a unique combination of methods, operating over varying temporal and spatial scales, to reconstruct the recent history of channel change. We use the temporally precise record of discharge measurements collected at the USGS streamflow gage to document changes in the shape of the channel over timescales as precise as the length of flood and over longer time scales spanning decades. In addition, we use the USGS discharge measurement notes to reconstruct the temporal sequence of changes in bed elevation and width. In addition to the USGS discharge measurement notes, we describe floodplain deposits in a few locations to understand the style, rate, and magnitude of both floodplain formation and channel narrowing. Both the USGS gage data and dendrogeomorphic analysis of floodplain deposits allows for the precise characterization of the history of channel and floodplain changes but only for specific sites, where the data records exist. Fortunately, the availability of aerial photographs back to 1938 provide the opportunity to extrapolate the style of channel change recorded at the USGS gage and in the floodplain stratigraphy over the entire downstream 100 km of the San Rafael River. Also, we use aerial imagery to quantify changes in reach scale processes such as channel narrowing, sinuosity, meander migration, and vegetation establishment. The integration of spatially robust and temporally precise methods provides a comprehensive picture of channel transformation during the previous 70 years.

### *A. Floodplain Stratigraphy*

We determined the rate and style of channel narrowing and floodplain formation by combining a novel technique of dating floodplain sediment by using the burial signals of individual tamarisk plants, and the interpretation of floodplain sediments in three trenches. When a tamarisk shrub is buried, the annual rings become narrower, vessels within the rings become larger, and annual transitions become less distinct (Friedman et al, 2005). Consequently, it is possible to interpret these anatomical changes to determine the exact year that a layer of sediment was deposited. By cross correlating among plants, it is possible to validate the interpretation of burial signals, thus providing a robust method for dating recent floodplain deposits.

We excavated three floodplain trenches on land owned by the Utah Division of Wildlife Resources. Figure 5 shows the location of the three trenches. We completed the first trench on the Hatt Ranch in spring 2009, the first Frenchman's Ranch trench in spring 2010, and the second Frenchman's Ranch trench in July 2010. The two trenches on Frenchman's Ranch are located directly across the river from each other, one on the left bank, and the other on the right bank (Figure 11). We opened the trenches by using an excavator and by using hand shovels. We surveyed the ground surface of each trench using an RTK GPS, and we mapped the floodplain stratigraphy on a scaled version of the ground surface and marked the intersection of the sediment layers on each tamarisk plant. Dendrochronology analysis of each tamarisk plant, using the methods described in Friedman et al (2005), was undertaken at the USGS Fort Collins Science Center under the supervision of Mike Scott.

The results presented in this report are for the Hatt Ranch trench. Recently, we received the dendrochronology results from the trench on the left bank at Frenchman's Ranch. In September 2010, we delivered six trees from the trench on the right bank at Frenchman's Ranch to the USGS Fort Collin Science Center dendrochronology laboratory, and the lab is currently analyzing these trees. Analysis of these trees is expected to be completed in spring 2011. Grain size analysis of sediment samples taken from a majority of the identified sedimentary deposits in the three trenches is completed, and the results will be incorporated in Fortney's master thesis.

### Frenchmans Ranch Trench – left bank

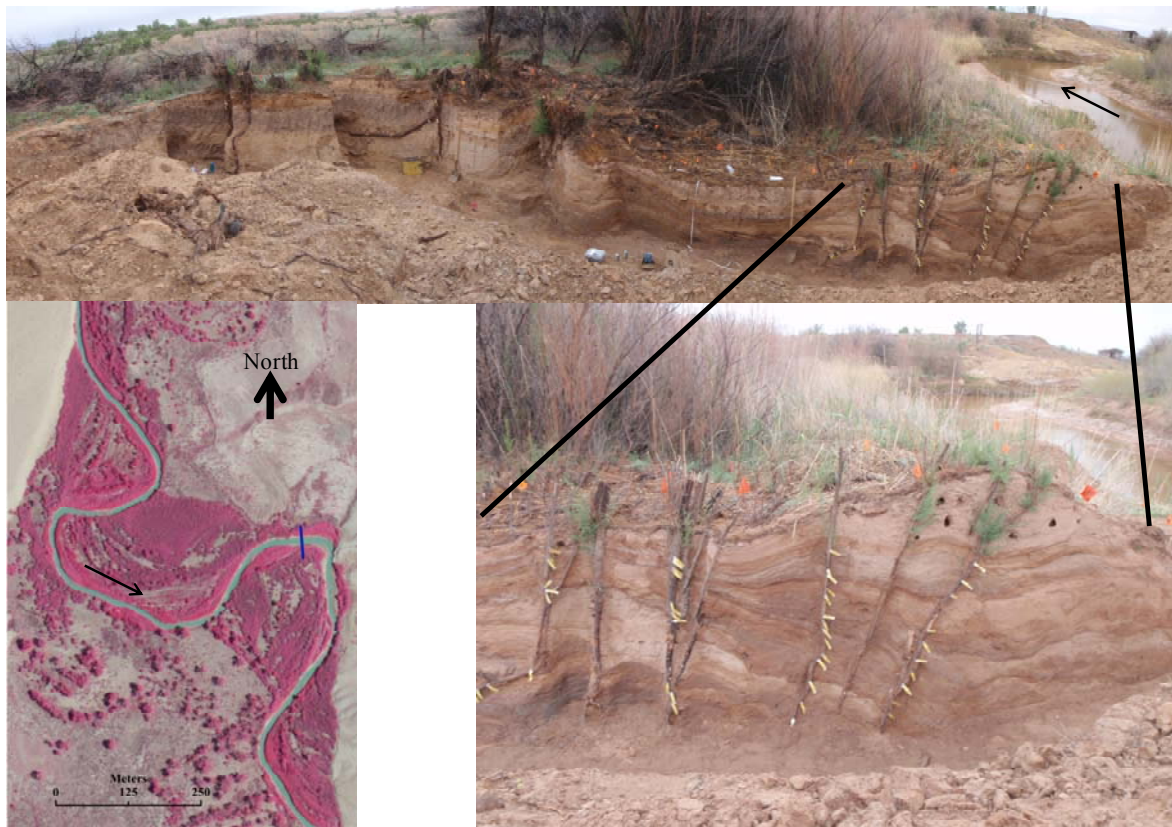


**Figure 11. Trench on left bank at Frenchman's Ranch. The aerial photograph in bottom right shows the location of both the left bank and right bank trenches. Bottom right photograph shows trees buried in silt and sand in a modern levee.**

#### ***B. Repeat Photography: Aerial Imagery and Oblique Ground Photographs***

By analyzing aerial photographs, we are able to extrapolate our understanding of the effects of flow reduction and vegetation establishment attained at specific sites over a much larger spatial area. Through the interpretation of aerial photographs, we are able to (1) quantify the spatial extent of floodplain formation that is discovered through stratigraphic interpretation of floodplain deposits, (2) quantify the rate and magnitude of channel narrowing over the entire lower river or where photo coverage exists, and (3) quantify additional plan form metrics such as meander migration and sinuosity. We have acquired eight series of aerial photographs that span a

period of 72 years. Table 7 lists relevant information for each photo series. Six of the eight photo series cover the entire lower 87 kilometers of the San Rafael River. The photos from 1962 and 1974 provide only partial coverage of the lower river: 59.7 km and 49.6 km, respectively.

In order to analyze historic aerial photographs, first the photos were georeferenced, which is the process of assigning a coordinate system to an image. We scanned the paper copy images at 1200 dpi (dots per inch) before georeferencing them in ERDAS Imagine 9.3. Thus far, we have georeferenced the photos (one of each stereo pair) from 1962, 1974, and 1985. The 2009 orthorectified imagery (1 meter resolution) was used as reference imagery during the georeferencing process. We used a combination of resampling and transformation techniques that provided the best positional accuracy. Acceptable root mean square error (RMSE) tolerances for each series of images varied, based on the spatial resolution of the input image. Uncertainty in positional accuracy will be assessed by comparing a high resolution field survey of known stable points to the same points in each photo series. Once the photos were georeferenced, we delineated the active channel in ArcGIS. We defined the active channel based on several criteria: (1) break in slope as observed in stereoscopic analyses, (2) relative absence of vegetative cover, (3) and change in sediment color. We divided the area of the active channel calculated for each photo series by the length of the channel centerline to determine the reach average active channel width (RAACW).

For this study, we also have access to high resolution (5 cm) natural color imagery of the entire lower river to augment interpretation of geomorphic changes. In August 2010, the Bureau of Reclamation (BOR), in collaboration with the Bureau of Land Management (BLM) and Utah State University (USU), photographed the entire length of the San Rafael River from a helicopter at approximately 450 meters above ground level. The Bureau of Reclamation is in the progress of mosaicing and georeferencing these high resolution photographs. We will use the 2010 imagery to map the spatial extent of various floodplain features. By producing a surficial geologic map of the alluvial valley, we will quantify the spatial extent of the floodplain features observed and characterized in the floodplain trenches.

An additional type of repeat photography is historical oblique ground photograph matching. Repeat oblique ground photos are useful in comparing current conditions to historical conditions in the channel and adjacent floodplain (Kondolf and Larson, 1995). In this report, we matched a present day photo of the old highway 24 bridge with a photograph acquired from the archived USGS gage records. By matching the historic photo taken at the USGS gage, we are able to reveal the extent of floodplain development or destruction, the type and density of cover of riparian vegetation community, change in channel width, change in bed elevation, and changes to the volume of stored sediment. Future matching of additional historic oblique ground photos will augment our understanding of geomorphic changes to the floodplain and channel.

### *C. USGS gage data*

Analysis of USGS gage data provides a temporally precise view of channel change and floodplain formation at the location of the measurement cross-section. Analysis of historic gage data provides insight into the adjustability of the bed, trends in aggradation or degradation, adjustability in the width of the channel, and adjustability in the shape of the channel in response to a range of discharges (Smelser and Schmidt, 1998). We analyzed data measured at the USGS stream gage for the entire period that the gage has been in operation. Prior to analyzing data from approximately 1450 discharge measurements, it was necessary to account for all datum shifts by acquiring and reviewing the level notes, station descriptions, and station analysis reports. Once the data were rectified to a common datum, which in this case was the datum of 2010 for the period between 1976-2010, and the datum of 1976 for the period between 1947-1976, then the results could be attributed solely to actual channel adjustment. In the results section of this report, we present an analysis of reconstructed cross sections, temporal sequence of minimum stream bed elevations (MINSBE), temporal sequence of width and width-to-depth, and hydraulic geometry.

#### *Reconstructed Cross Sections*

Reconstructed cross sections illustrate, in 2 dimensions, the style and magnitude of changes in the geometry of the channel through time. In addition, the reconstructed cross sections indicate bed elevation changes if they have occurred. Between 1947 and 1976, the USGS measured discharge at many locations, ranging from 3.2 km upstream from the gage (Interstate 70) to 3.2 km downstream from the gage, but commonly within approximately 300 m of the gage. In order to avoid any differences that these different locations might cause in channel geometry, only discharge data measured at one location, the abandoned cableway, located approximately 150 m downstream from the old highway 24 bridge (Figure 12), were used. Also, only measurements that best depict bankfull channel width were used. We plotted data collected during the measurement of a range of discharges between 817 ft<sup>3</sup>/s and 2370 ft<sup>3</sup>/s, all of which are greater than the 1.1-year recurrence flood (approximately 700 ft<sup>3</sup>/s).

Various positions where the USGS gage has been located are identified in Figure 12. The gage has been moved six times. Between 1909 and 1976, the gage was located near the old Highway 24 bridge on the Hatt Ranch, except for two years between 1945 and 1947 when the gage was located approximately 200 m downstream from the old Highway 24 bridge. Since 1976, it has been in the same location, approximately 150 m upstream from the current Highway 24 bridge. At the present gage location, the USGS measures flood discharges from the Highway 24 bridge instead of at the cableway. Neither the datum of 1909-1920 or of 1945-1947 is related to the datum of 1947-1976. Likewise, the datum prior to 1976 is not related to the datum at the current gage location. For these reasons, it is only possible to compare historic cross section for the period 1947-1976.

### *Rating Relations*

Rating relations express both the shape and hydraulic character of a channel reach (Dunne and Leopold 1978). Rating shifts are a reflection of either a datum adjustment or changes in the channel cross section, either scour or fill, or widening or narrowing (Rantz, 1982). Since all datum adjustments have been accounted for in this study, and the gage heights rectified, then the shifts in the rating relations indicate actual channel adjustments. All measurements affected by ice were removed from the data used in construction of the rating relations, since backwater caused by ice creates an anomalous high water elevation.

### *Time Series of Thalweg Elevation*

By analyzing the time series of minimum stream bed elevation measurements (MINSBE), it is possible to quantify the magnitude and timing of bed elevation change. This analysis provides the necessary temporal resolution to decipher the effect of individual flood events on the elevation of the bed and also determine periods of adjustment occurring over large time scales. Furthermore, comparison of individual hydrographs to the MINSBE time series and velocity time series provides the opportunity to evaluate how the streambed responds to the progress of a flood i.e. rising stage, peak(s), and falling stage. We followed the methods described by Smelser and Schmidt (1998) and subtracted the maximum depth of each discharge measurement from the rectified gage height. Before plotting the computed thalweg elevations we exclude measurements affected by ice were. Also, we did not plot data for the time period between 1945 and 1947, because the datum for this period cannot be related to the datum subsequent to 1947. Finally we converted bed elevations measured in the local coordinate system used by the USGS to the global elevation system. Thus we report the elevation of the bed and water surface in meters above sea level, beginning in 1947.

### *Time Series of Width and Width-to-Depth Ratio*

The temporal sequence of width-to-depth and width provide sufficient temporal resolution to determine the precise year in which changes in channel width occurred. In order to characterize how the width of the “active” channel changed over time we excluded both low flows that didn’t fill the active channel, and large floods that possibly spilled over the banks of the active channel and kept data points for all discharges between 250 and 1000 ft<sup>3</sup>/s. However, we did not filter the data by measurement location, so the width time series may include measurements taken at both bridges, various cableways, the bedrock riffle located approximately 400 m downstream from the current gage, or various other locations.

### *Hydraulic Geometry*

The at-a-station hydraulic geometry is a statistical method that shows how flow variables vary with discharge (Leopold and Maddock, 1953). Hydraulic geometry provides a quantitative description of how the channel geometry adjusts to changing discharges in one location by using power models to relate discharge to channel geometry (depth and width) and velocity. The general forms of the power law equation for width, depth and velocity are:

$$w=aQ^b$$
$$v=kQ^m$$
$$d=cQ^f$$

The hydraulic variables  $w$ ,  $v$ , and  $d$  are top width, mean depth, and mean velocity of the cross section, respectively. The exponent's  $b$ ,  $m$ , and  $f$  represent the slopes of the power models. The magnitude of the exponents represents the rates of change of each variable with respect to the independent variable discharge. The coefficients  $a$ ,  $k$ , and  $c$  represent the y-intercepts. Since the law of conservation of mass states that  $Q=wk d$ , then the product of the coefficients'  $a$ ,  $k$ , and  $c$  should equal unity. Likewise, the sum of the exponents  $b$ ,  $m$ , and  $f$  should also equal unity. Prior to analyzing the hydraulic geometry relationships at the USGS gage 09328500, we filtered all of the data based on measurement location. Before creating the hydraulic geometry relationships we removed all of the measurements taken at both bridges since a bridge unnaturally constricts the width of the channel especially at high stream flows. In addition, we excluded measurements taken at the bedrock riffle and measurements affected by ice.

It should be noted that limitations, in addition to measurement location, may result in a misrepresentation of the historical shape of the channel. First, the USGS gage 09328500 is located on the Hatt Ranch where channel modification, and activities that influence the shape of the channel, have been occurring for most of the time the gage has been in operation. The owners of the ranch constructed two different diversion dams at different times, constructed levees to control the migration of the river, and straightening the river by cutting off two large meanders. Also, two bridges are currently located on the ranch, one where the old state highway 24 crossed the river and one where the current highway 24 crosses the river. Second, the quality of the measurements due to human error and the use of different velocity meters, both introduce error in the hydraulic geometry relationships. Third, because the USGS gage is located in an extensively modified reach and differs in character from a large portion of the lower river, the hydraulic geometry relationships developed for data collected at the USGS gage may not apply to more natural parts of the river channel. Despite the contribution of multitude of sources of error, hydraulic geometry relationships provide a means to interpret the response of the river channel to changing discharges during the past (Alexander et al, 2009). Finally, an understanding of how the shape of the channel has changed over time allows for the characterization of changes in fish habitat.

#### ***D. Longitudinal Profile***

Channel gradient is one of four elements that compose the structure of the geomorphic template of the channel. Consequently, gradient contributes to the mosaic of fish habitat in the San Rafael River. A survey of the longitudinal profile of the river assists in characterizing the composition of fish habitat along the longitudinal gradient of the lower river and assists in determining underlying causes for the current distribution of fish habitat.

In early November 2010, we completed a survey of the water surface elevation and bed elevation of the entire lower river (approximately 90 km) between the San Rafael Reef and the confluence with the Green River (Figure 5). We collected each point using a Real Time Kinematic Global Positioning System with a predefined instrumental horizontal precision of 1.5 cm and vertical precision of 3 cm. We collected points approximately every 100 m, for a total of 3500 surveyed points. Results from the longitudinal survey will be used (1) as baseline data for future geomorphic, ecologic, and restoration studies, (2) to determine the effect of the Hatt Ranch diversion on channel slope both in the upstream and downstream directions, and (3) identify lithologic and hydraulic controls. In addition, we will combine the habitat characterization study conducted by Dr. Budy's lab with the results of the longitudinal profile survey, in order to better understand the factors responsible for the present distribution and quality of fish habitat in the lower river. Furthermore, this information will be important for determining the suitable reaches to concentrate rehabilitation efforts.

#### ***E. Additional Activities***

We plan to sample the bed material of the lower river in spring 2011. The sampling scheme will entail describing the distribution of sediment sizes along the entire lower river. Since most of the river bed is sand and mud, it should be sufficient to characterize these long reaches of fine material by collecting grab samples approximately every 10 km. We will use information about the location of gravel riffles gathered during previous surveys to choose the appropriate spacing and frequency of pebble counts. The combination of volumetric grab samples and pebble counts will sufficiently describe the distribution and type of sediment that presently occurs in the bed of the lower San Rafael River.

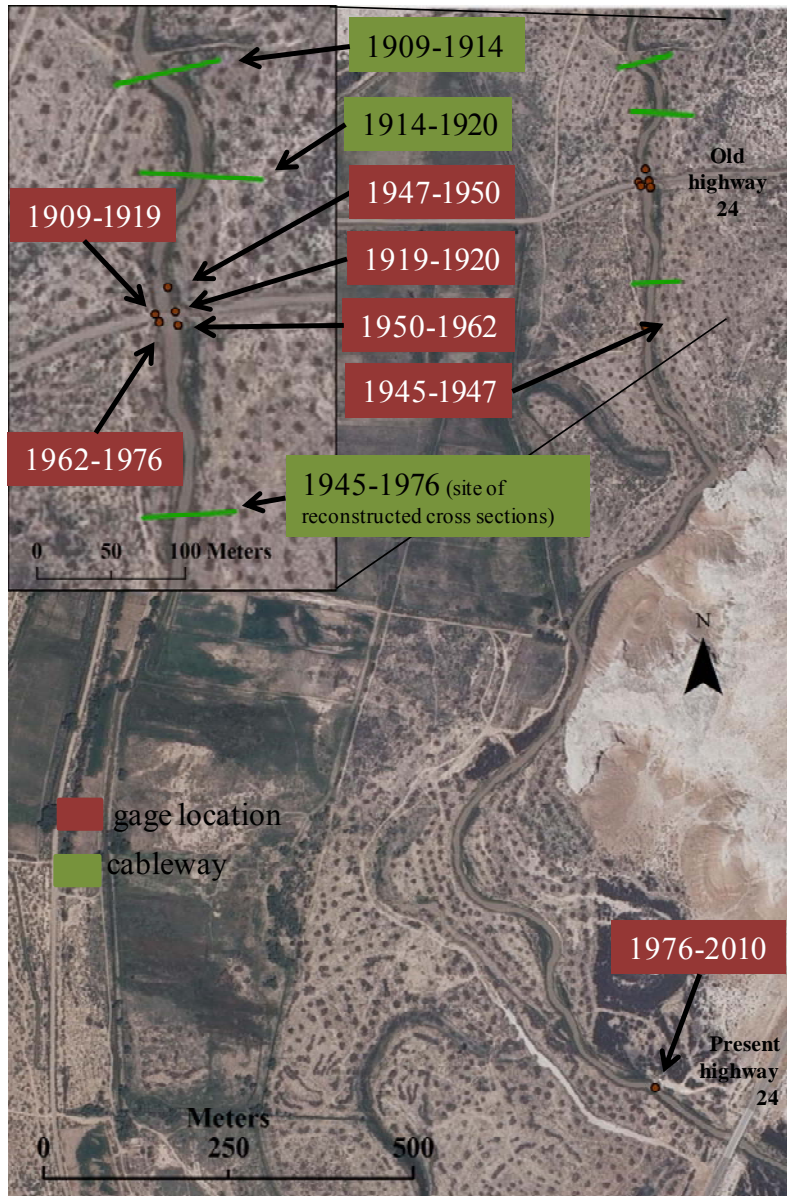


**Figure 12.** On this 2009 aerial photograph are identified both the abandoned cableways used to measure high streamflow and the various gage locations. The USGS moved the gage five times between 1909 and 1976 and moved again in 1976. Since 1976, it has been in the same location, approximately 150 m upstream from the current Highway 24 bridge. Currently, the Highway 24 bridge is used to measure flood discharge.

## **VI. Results: Channel Transformation on Hatt Ranch**

### *Turn of the 20<sup>th</sup> century*

At the turn of the 20<sup>th</sup> century, the San Rafael River on the Hatt Ranch was characterized by multiple threads, numerous bars, and a low width-to-depth ratio. The gentle sloping, non-cohesive banks as shown in a historic oblique photo taken at the turn of the century (Figure 1) were easily eroded during floods. The connection between the mainstem and floodplain provided opportunities for native fish to access food resources and refugia during floods, and for riparian plants to fall into the channel. Annual floods reorganized the template of the river. The historic photograph in Figure 1 also shows a riparian zone consisting of a cottonwood and willow.

The bed elevation exhibited considerable variability between 1909 and 1920; however, there is no overall trend of degradation or aggradation during this period. The standard deviation and variation of the thalweg elevation was 0.9 m and 0.8 m, respectively (Table 3). In some instances, snowmelt floods scoured on the rising limb and filled on the falling limb. For example, during the snowmelt floods of 1917 and 1918, the bed scoured on the rising limb, approximately 1.2 meters and 1 meter, respectively, and the stream bed filled during the falling limb of both years. In 1917, however, the bed did not return to the pre-flood elevation until October. In contrast, in 1918, the bed resumed the pre-flood elevation upon the recession of the snowmelt flood. Conversely, the bed filled on the rising limb and scoured on the falling limb during the snowmelt floods of 1912 and 1913 (Figure 13). In summary, the order of scour and fill varied for different snowmelt floods.

Annual scouring and filling of the bed during the early 20<sup>th</sup> century, however, was not always achieved by a snowmelt flood or even a monsoon flood. In fact, Figure 13 shows that the bed scoured and filled during time spans when there was no significant flooding. For example, the bed varied in elevation by 3.25 m over the course of nearly two years, between June 1916 and March 1918. During the peak of the snowmelt floods of 1916 and 1917, the bed scoured. Commencing with the recession of the 1917 snowmelt flood, the bed filled 3.25 meters over the course of 10 months until March 1918, when it returned to the elevation it was in 1916.

In addition to large variability in bed elevation, channel width also varied significantly. The mean width of the channel was 30.9 m and the standard deviation was 4.9 m during the period 190-1920 (Table 4). Also, Figure 14 shows that the first period of record exhibited a high width-to-depth ratio, (Table 5). In general, the data for the earliest period of time analyzed in this study (1909-1920) shows that the San Rafael River exhibited great variability in both width and bed elevation. In conjunction with easily erodible banks and a low width to depth ratio, channel variability maintained complex heterogeneous habitat for native fish.

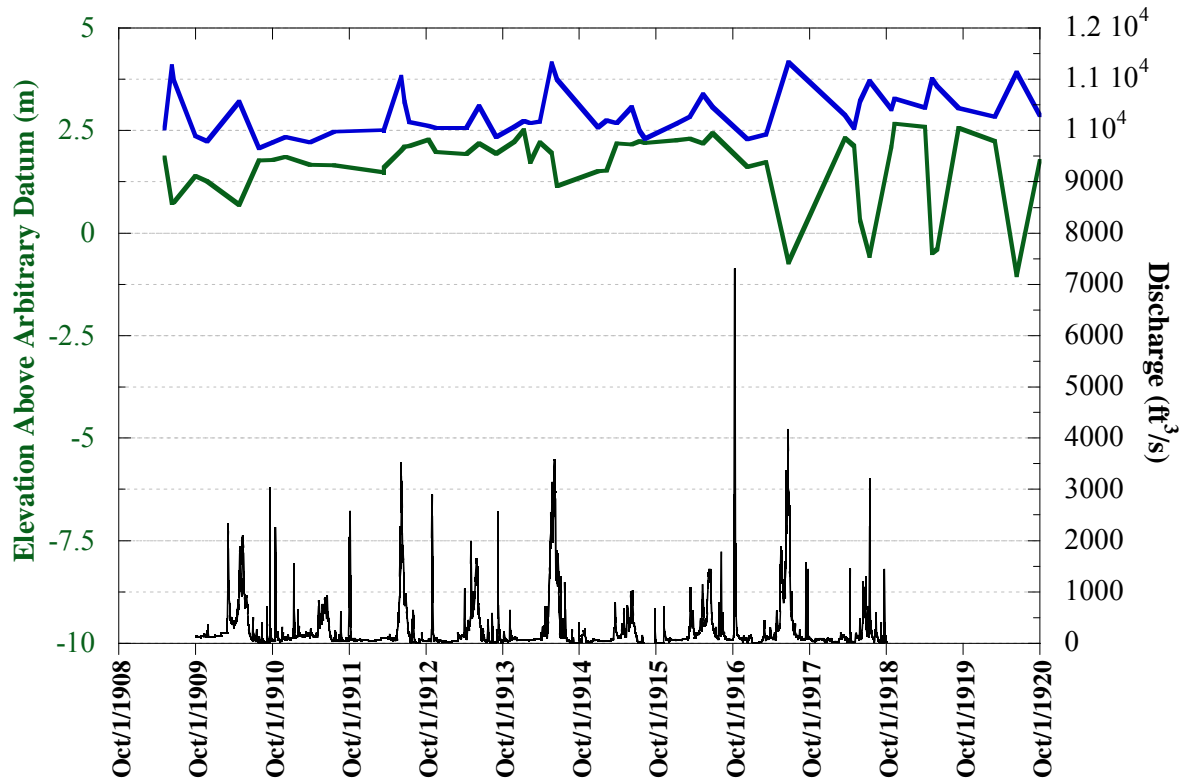


Figure 13. Time series of MINSBE, water surface elevation and discharge between 1909 and 1920.

Table 3. Statistics for each time period of adjustment shown in the MINSBE analysis.

Statistic	1909-1920	1947-1952	1952-1958	1958-1965	1965-1976	1976-1983	1983-2008
Minimum	-1.0	1259.0	1257.7	1257.4	1257.5	1256.0	1254.5
Maximum	2.7	1259.8	1259.3	1258.5	1258.4	1257.5	1257.0
Points	53.0	208.0	118.0	116.0	151.0	77.0	211.0
Mean	1.6	1259.3	1258.6	1257.7	1257.9	1257.1	1256.4
Median	2.0	1259.3	1258.6	1257.7	1257.9	1257.2	1256.4
Std Deviation	0.9	0.2	0.4	0.2	0.2	0.3	0.3
Variance	0.8	0.0	0.2	0.0	0.0	0.1	0.1

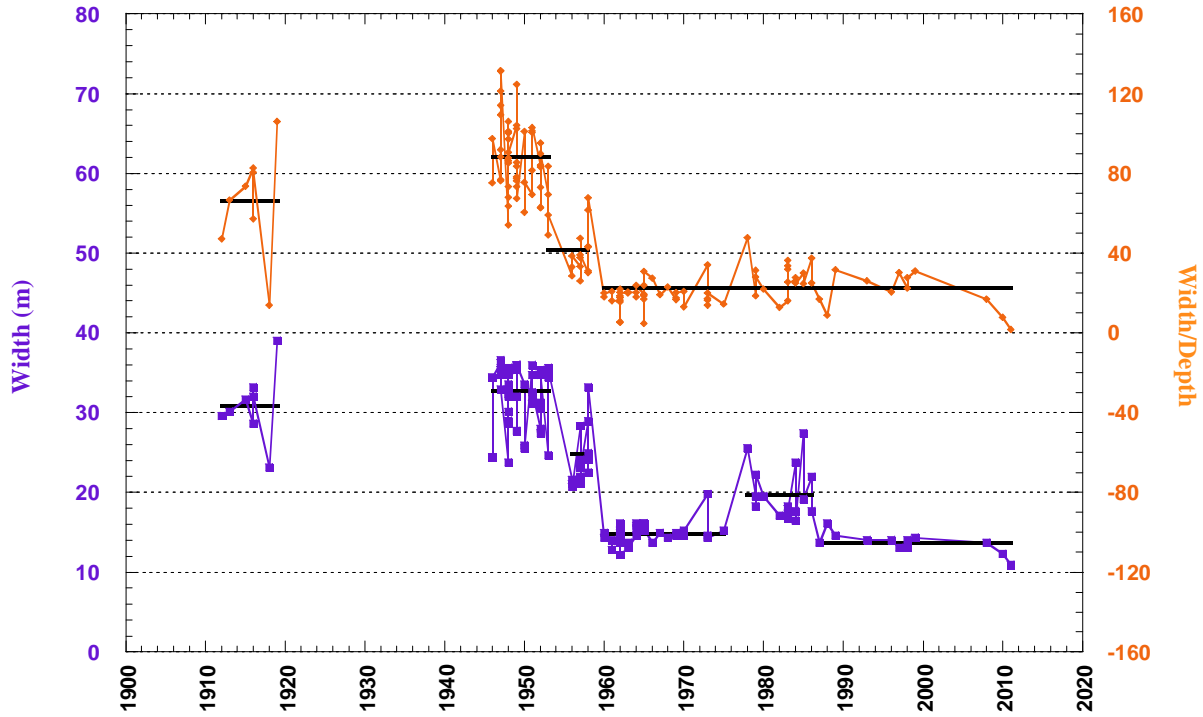


Figure 14. Time series of width and width-to-depth ratio for entire period of record

Table 4. Statistics for each of six time periods of adjustment shown in the width time series.

Statistic	1909 to 1920	1945 to 1953	1953 to 1958	1959 to 1976	1976 to 1986	1987 to 2010
Minimum (m)	23.2	23.8	20.7	12.2	16.5	11.0
Maximum (m)	39.0	36.6	33.2	19.8	27.4	16.2
Points	8.0	53.0	14.0	40.0	18.0	12.0
Mean (m)	30.9	32.8	24.9	14.9	19.7	13.7
Median (m)	30.9	34.4	23.6	14.6	18.3	13.9
Std Deviation (m)	4.5	3.6	4.3	1.2	3.2	1.3
Variance (m)	20.0	12.8	18.7	1.5	10.2	1.6

Table 5. Statistics for each of four periods of adjustment periods of the width-to-depth ratio.

Statistics	1909 to 1920	1945 to 1953	1953 to 1958	1958 to 2010
Minimum	13.9	54.3	26.0	6.0
Maximum	106.2	131.6	67.8	47.7
Points	8	51	16	70
Mean	66.0	88.2	41.8	22.4
Median	70.0	85.6	38.9	20.4
Std Deviation	27.5	18.2	12.4	6.9
Variance	757.3	331.7	153.9	48.3

### *1930s and 1940s*

During the 1930s and 1940s, the geomorphic template of the river did not differ significantly from the earlier part of the 20<sup>th</sup> century. The annual snowmelt flood, despite a reduction in its magnitude and duration (Figure 38 in Appendix), continued to maintain a wide channel. Aerial photographs taken in 1938 (Figure 17) show a wide, multi-threaded channel with numerous bars and a riparian community dominated by willow and cottonwood. The river presumably continued to provide native fish with abundant, diverse habitat, including a connection between the channel and the floodplain. Despite the relatively unchanged nature of the channel, human modification of the alluvial valley on the Hatt Ranch may have begun to alter the natural behavior of the channel. Agriculture on the west side of the alluvial valley confined the river to the east side of the valley. 1938 aerial photographs indicate a small diversion dam was in place by this time.

Results from several analyses indicate the channel in the 1930s and 1940s was similar in width to the channel in the early 20<sup>th</sup> century. A photo of the old Highway 24 bridge, taken prior to 1938 (Figure 16), shows that the river extended beyond both bridge piers, which span a distance of approximately 30 meters. Unfortunately, we do not know the streamflow at the time the photograph was taken, so we do not if the stage was low or high. In 1938, the reach average active channel width (RAACW) for a 10-kilometer reach upstream from Hatt Ranch was 51.7 m (Figure 15 and Table 6).

Both, the average bankfull width of the channel, and the width-to-depth ratio were greater for the time period 1945-1953, than for the time period 1909-1920. Mean “active” channel width for the two time periods, 1945-1953 and 1909-1920, was 30.9 m and 32.8 m, respectively. A greater number of data points for the period 1945-1953 may have caused an increase in channel width. Variability in the width measurements however, decreases for the second time period. Furthermore, variability in the elevation in the bed also decreased. Standard deviation of thalweg elevation for the period 1909-1920 was 0.9 m, which is four times larger than the standard deviation of 0.2 m for the subsequent period 1947-1952 (see Table 3). Lower magnitude floods during the period 1947-1952 may be responsible for the lower variation in bed elevations during this time period.

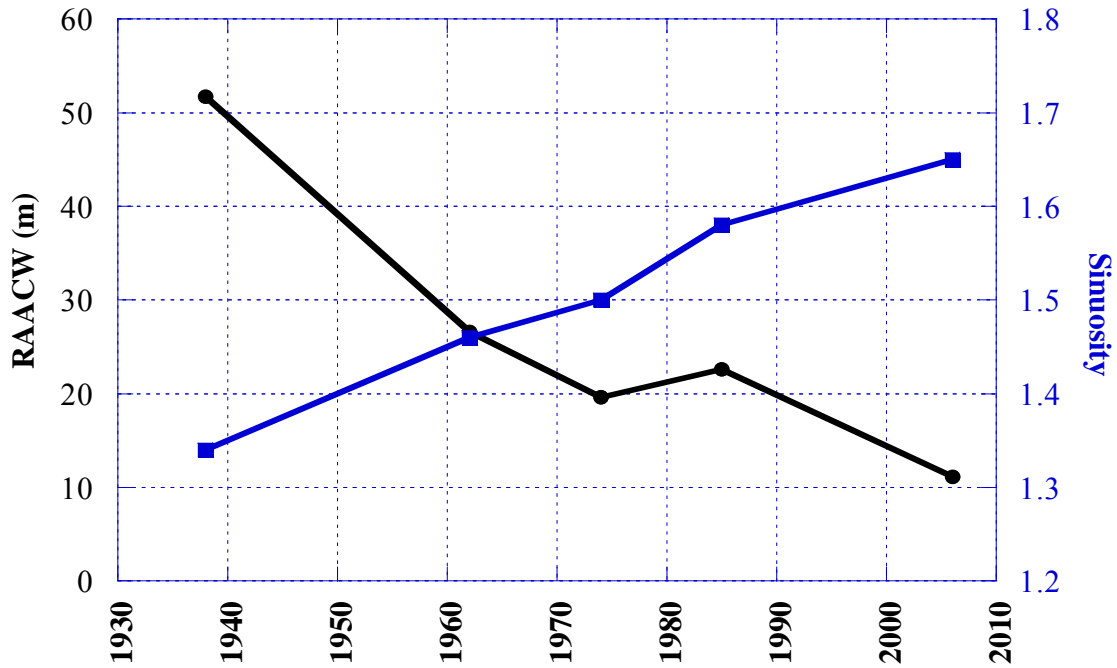
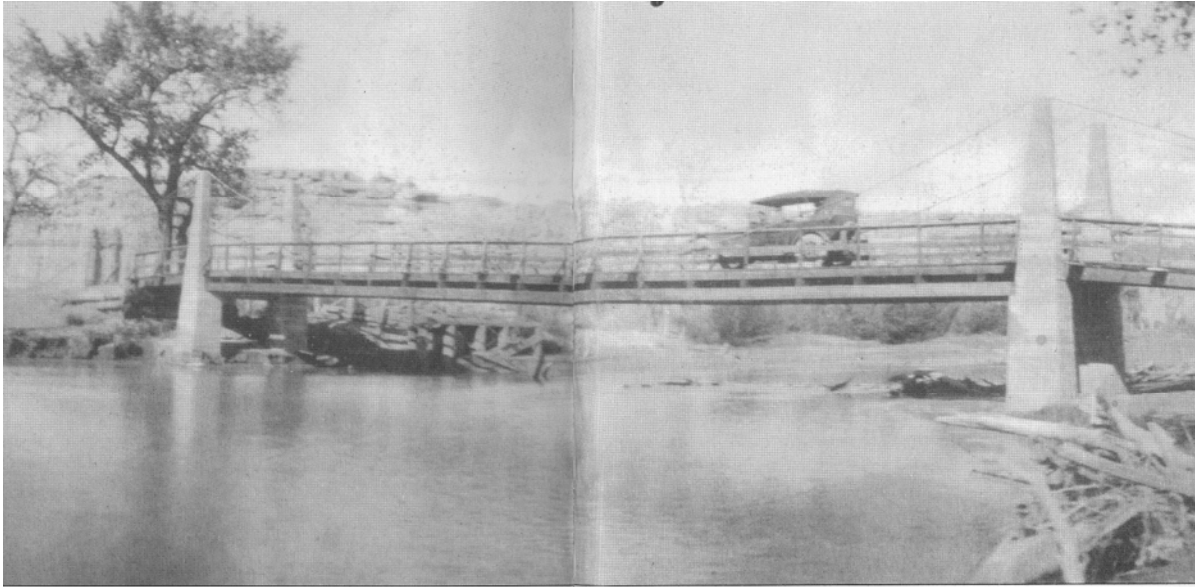


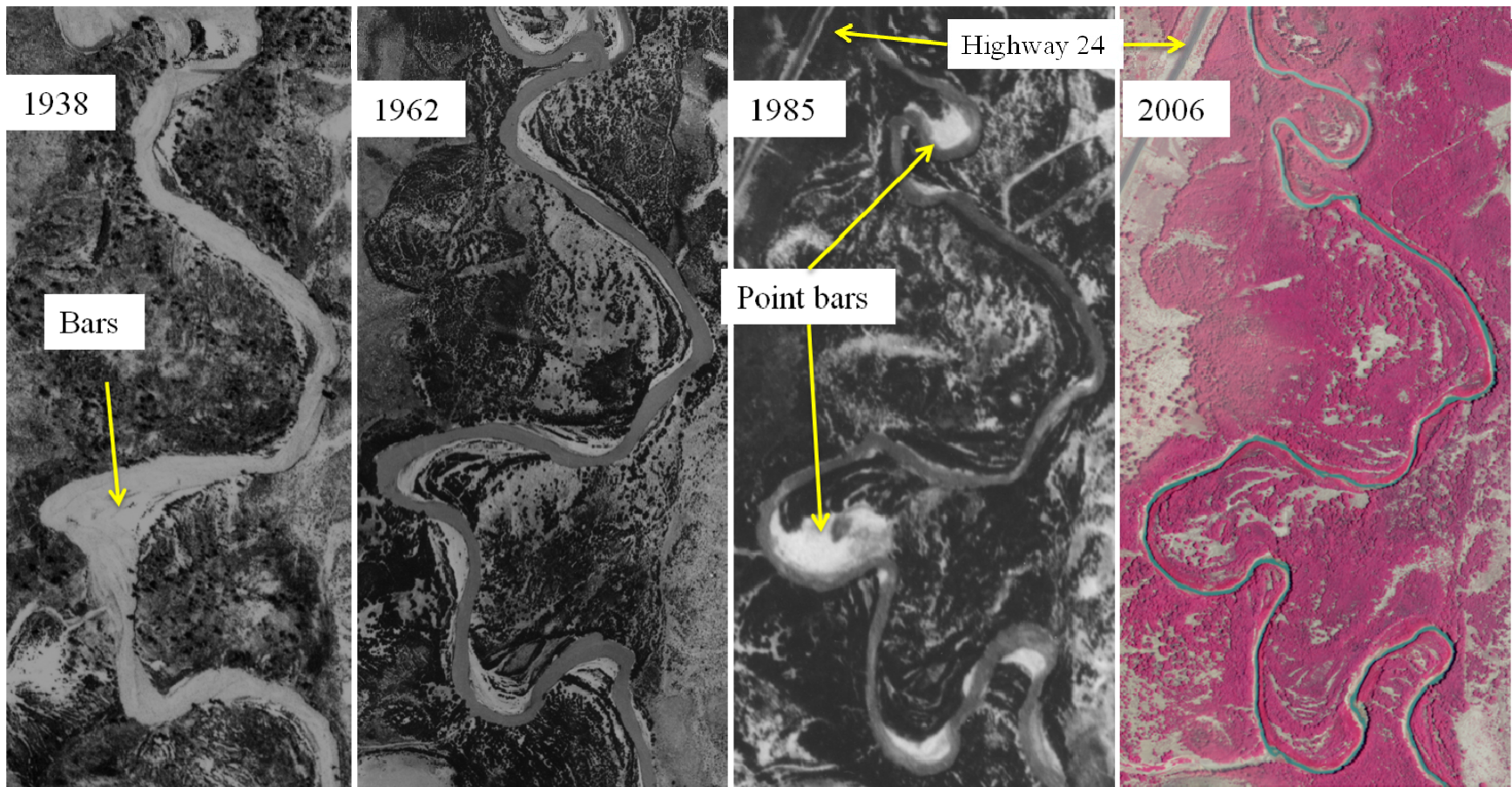
Figure 15. Results from plan form analysis of 10 kilometer reach upstream from Hatt Ranch

Table 6. Results from analysis of aerial photographs in 10-kilometer reach upstream of Hatt Ranch

Year	Area (km <sup>2</sup> )	Centerline Length (m)	RAACW (m)	Percent Change	Narrowing Rate (m/y)	Sinuosity **
2006	0.11	10000	11.1	-51%	0.5	1.65
1985	0.22	9549	22.6	15%	-0.3	1.58
1974	0.18	9097	19.6	-26%	0.6	1.50
1962	0.23	8827	26.6	-49%	1.0	1.46
1938	0.42	8117	51.7			1.34



**Figure 16. Comparison of two photographs taken of the San Rafael River at the old Highway 24 bridge on Hatt Ranch, looking upstream. Top photo was taken sometime before 1938 (precise date is unknown). Bottom photo, taken in 2010, shows a newer bridge located in front of the original bridge. The channel in the 2010 photograph is obscured by grasses and other vegetation on the floodplain. The active channel is not noticeable, because it is far below the floodplain features seen in the photo, which indicates that the channel has both incised and narrowed and the floodplain has aggraded.**



**Figure 17. Comparison of aerial photographs for a short reach downstream of the Hatt Ranch. Since 1938 the channel has narrowed considerably. Point bar creation in the 1985 photo is most likely a result of the large snowmelt floods in 1983 and 1984.**

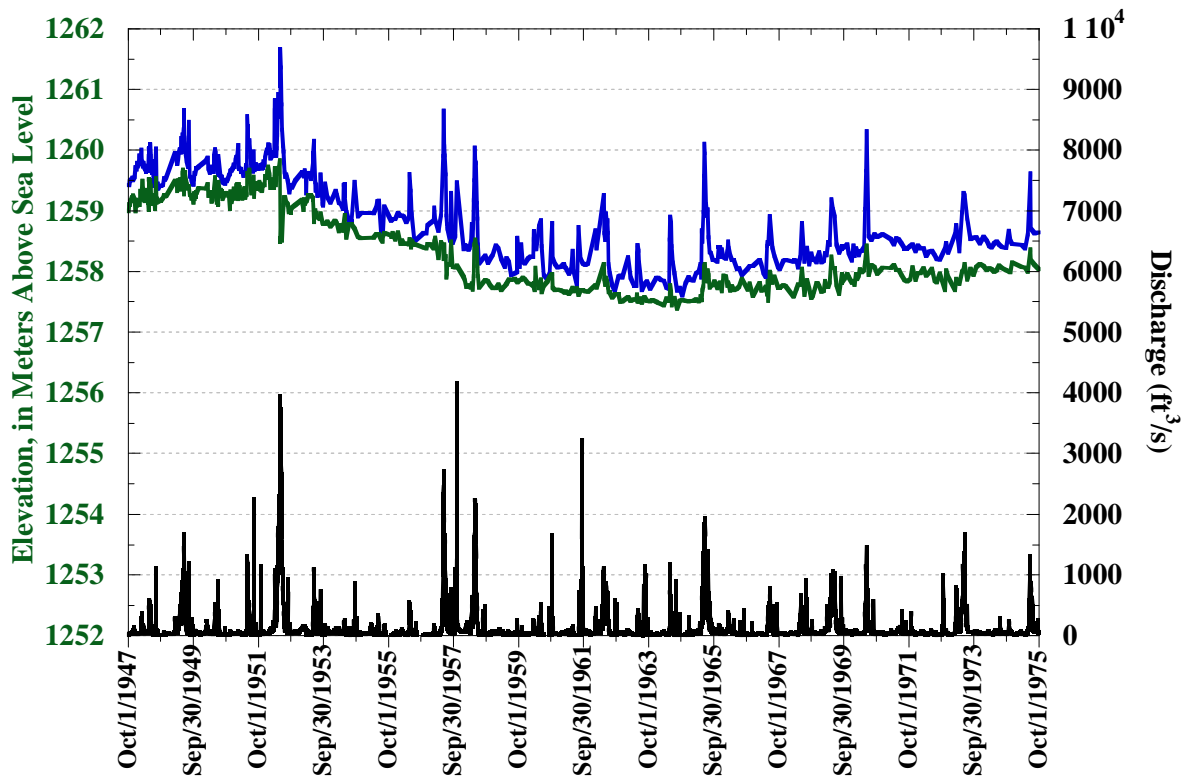


Figure 18. Time series of MINSBE, water surface elevation and discharge between 1947 and 1976.

### 1950s

The decrease in the duration and magnitude of the snowmelt flood (Figure 39 in Appendix) and the increase in the density of riparian vegetation contributed to significant geomorphic change in the 1950s. Aerial photographs taken in 1952 (Figure 19) depict the San Rafael River in a state that appears very similar to the aerial photographs of 1938. For example, the 1952 photos show that the channel contained numerous small bars and un-vegetated point bars, and was comprised of multiple threads in places. Also, changes in the riparian community are not evident in the 1952 aerial photographs (Figure 19), however, dendrogeomorphic evidence suggests that tamarisk established in the San Rafael prior to 1957. It is possible that the 1952 flood, which occurred just months before the photos were taken and contained the second biggest snowmelt peak and third largest snowmelt runoff volume in history (Table 1), reset the template of the river. Despite these observations that the San Rafael River was not different than previous decades, we know, based on the results from several analyses that the river narrowed and incised during the 1950s. The changes to the geomorphic template, described in detail below, certainly impacted the distribution and quality of habitat, and began a trajectory of change that presumably negatively impacted the native endemic fish.

The snowmelt flood of 1952 initiated a wave of incision, from which the bed has still not recovered (Figure 18). Not only did the 1952 snowmelt flood cause a net decrease in the elevation of the bed but the flood also shifted the position of the thalweg and filled a portion of the channel along the right bank (Figure 20). The appendix contains figures showing the cross sectional changes at the abandoned cableway during the progress of five additional snowmelt floods: 1949, 1957, 1958, 1962, 1965. Two days before the flood peak, the channel scoured suddenly along the left half of the channel, approximately 1.2 m, and filled in the right half of the channel. On June 4, the peak of the snowmelt flood, as the water overtopped the channel's banks, the velocity decreased and the channel filled. The USGS measured a total width of 1126 ft on June 4 both at the cableway and by wading in the floodplain. It was noted on the discharge measurement survey form for June 4 that "the water was up to the foot rest on the gaging car."

The fastest rate of incision occurred between 1952 and 1958, when the bed scoured approximately 1.5 m, at a rate of approximately 0.2 meter/year. Following the scouring event of 1952, incision steadily progressed between 1952 and 1956, a period characterized by very short duration, small magnitude snowmelt floods (the largest is approximately 1200 ft<sup>3</sup>/s) and an absence of any significant warm season floods (the largest is approximately 800 ft<sup>3</sup>/s). During the snowmelt floods of 1953 and 1956, which were much smaller in comparison to the 1952 flood, the bed filled during the rising limb, then scoured at the peak of the flood. The bed filled again but not back to the pre-flood elevation, thus contributing to the progress of incision.

The 1957 and 1958 snowmelt floods, punctuated the short period of progressive incision between 1952 and 1956 by causing different types of bed fluctuations. The snowmelt flood of 1957, which was not a particularly large flood behaved differently than the floods of 1953 and 1956 yet produced the same net result, one of bed lowering. The bed scoured during the final falling limb to an elevation approximately 0.6 m lower than the pre-flood elevation. On the other hand, the snowmelt flood of 1958 merely filled the bed temporarily, but did not cause any overall change in the bed elevation. Instead, the 1958 flood expanded the channel by eroding the recently aggraded banks (Figure 34 in Appendix). Consequently, the 1958 snowmelt flood restored the width of the channel to approximately the same width that existed in the early 1950's. The 1958 snowmelt flood behaved differently than the snowmelt floods of 1952, 1953 and 1957, yet similar to the snowmelt floods of 1912 and 1913. Instead of scouring during the rising limb or at the flood peak, the bed filled approximately 0.7 m during the rising stage and achieved a maximum thalweg elevation at the peaks of discharge and velocity. As the 1958 flood receded, the bed scoured approximately the same magnitude during the falling stages, thereby returning the bed to its pre-flood elevation.

Channel narrowing occurred in conjunction with incision in the mid 1950s. Evidence from dendrogeomorphic analysis of floodplain sediments indicates significant narrowing occurred prior to 1957. Since the entire excavated trench, also shown in cross section view in Figure 23, is

located within the active channel of the 1938 georeferenced photo (Figure 24) it can be inferred that a significant portion of the package of sediment in blue was deposited sometime between 1938 and 1957. Indeed, plan form analysis reveal that the fastest rate of channel narrowing, of any period bracketed by photos, occurred between 1938 and 1962, during which time the RAACW decreased by nearly 50%, from 51.7 m to 26.6 m (Figure 15 and Table 6). By comparing the results of the planform analysis to the temporal sequence of width measured at the USGS gage, it is assumed that most of the decrease in RAACW occurred during the same time that the major shift in channel width occurred at the USGS gage. Prior to 1953 the “active” channel width varied significantly, but appeared to be stable. Then in 1953, the “active” channel width decreased by 24% (Figure 14). Therefore, it can be assumed reasonable that the majority of narrowing indicated by the decrease in RAACW occurred mostly in the 1950s. Also, the width-to-depth ratio decreased 53% during the 1950s, from a mean of 32.8 m during the period 1945-1953 to 24.9 m during the period 1953-1958.

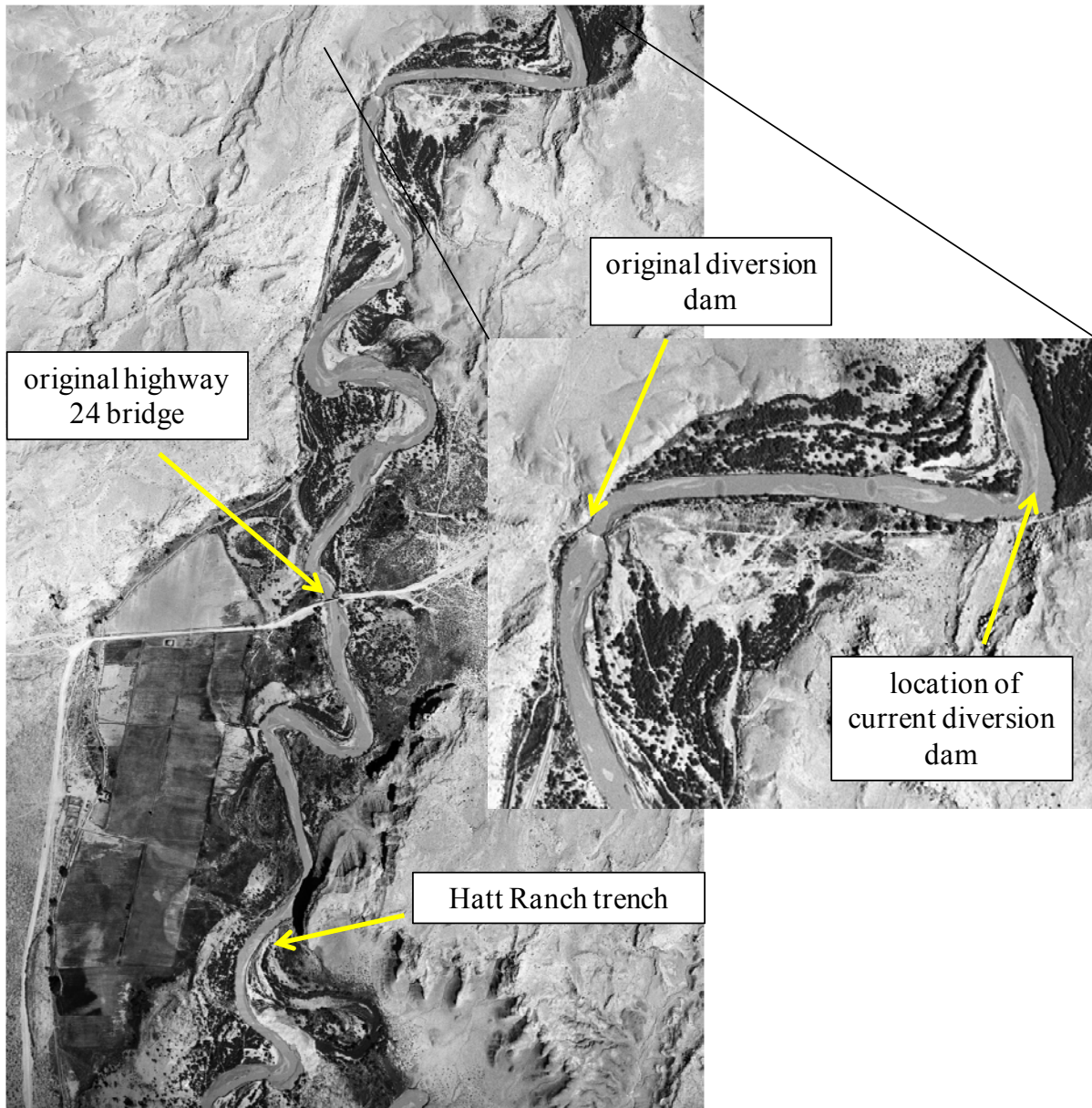


**Figure 19. 1952 aerial photo of vicinity of Hatt Ranch. Shown in the magnified inset is the location of the diversion dam in place before the 1952 photo was taken, and the location of the current, much larger diversion dam (built after 1952). Photo shows a wide channel with numerous bars and abundant bare floodplain surfaces.**

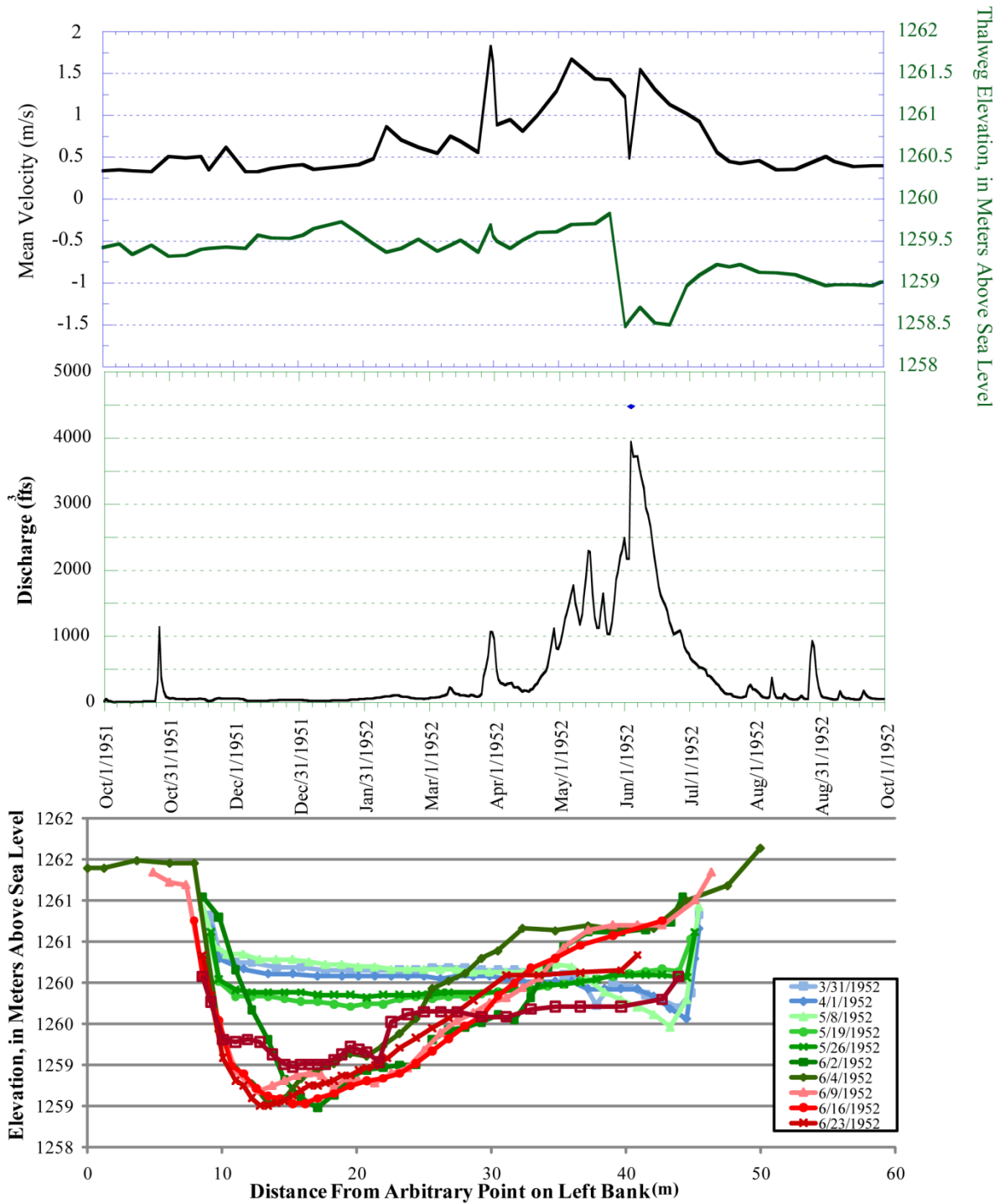


**Figure 20. Cross sections and time series of discharge, MINSBE and velocity during the progress of the snowmelt flood of 1952. Cross sections in shades of green were measured during the rising limb of the flood hydrograph. Cross sections in shades of red were measured during the falling limb.**

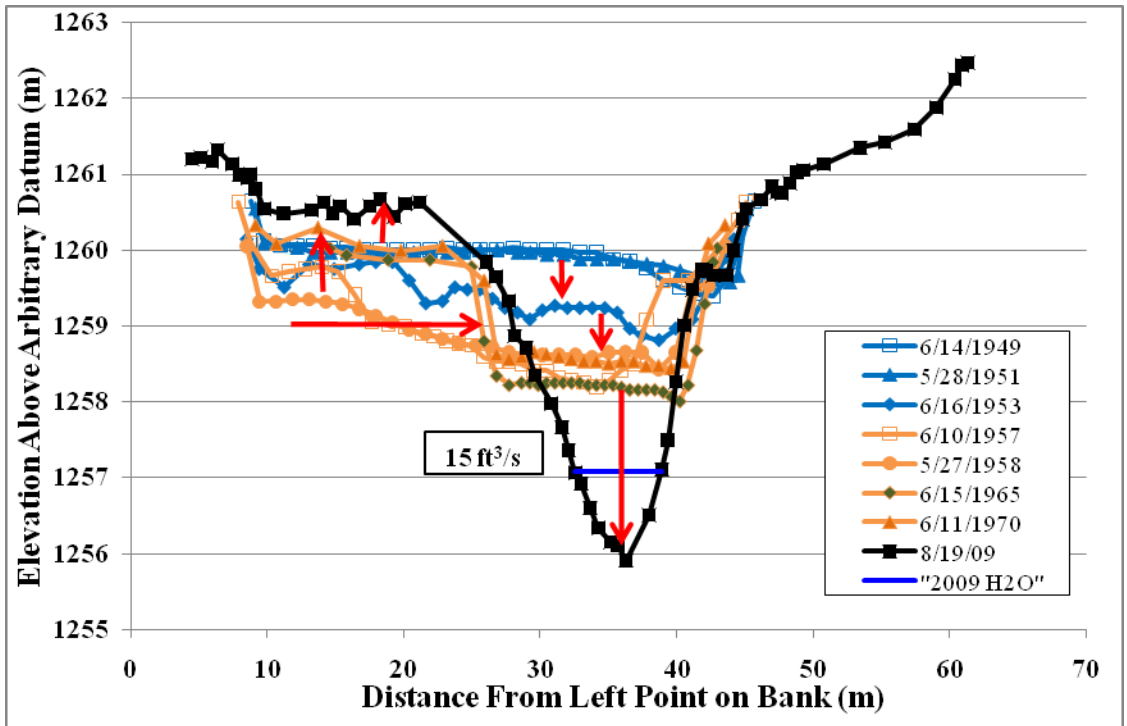


Figure 21. Reconstructed cross sections at the original location of the USGS gage (09328500), approximately 150 m downstream from the old Highway 24 bridge. Colors are correlated with colors of sediment packages in Hatt Ranch trench shown in Figure 23

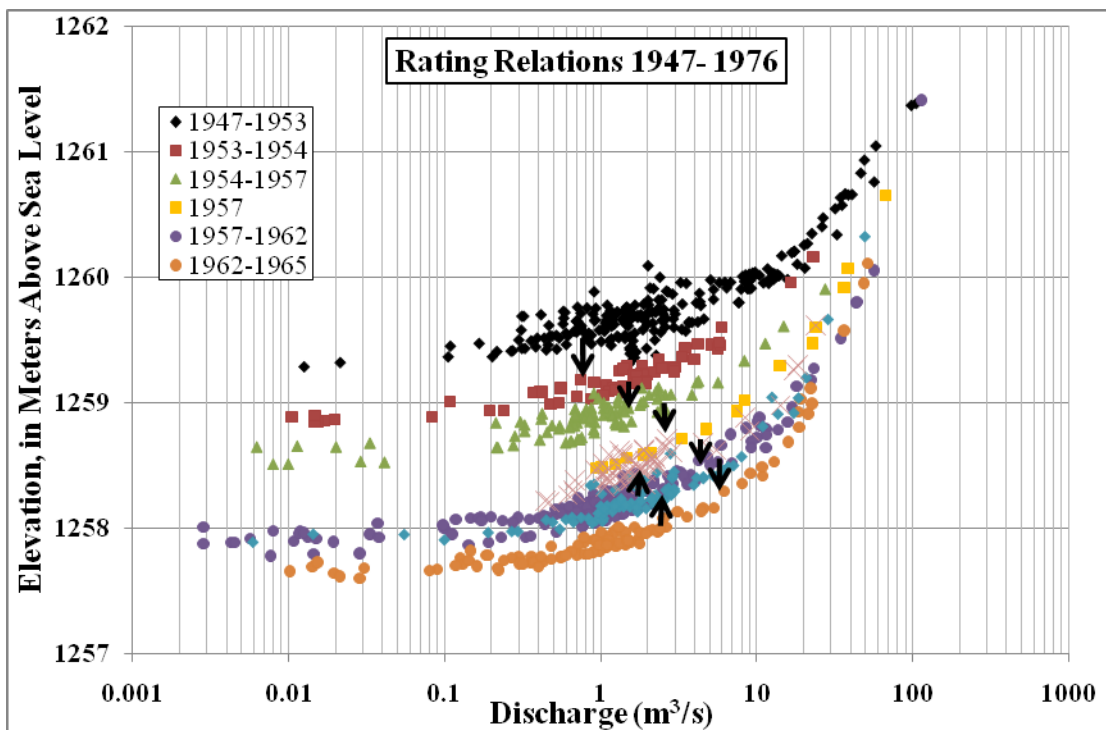
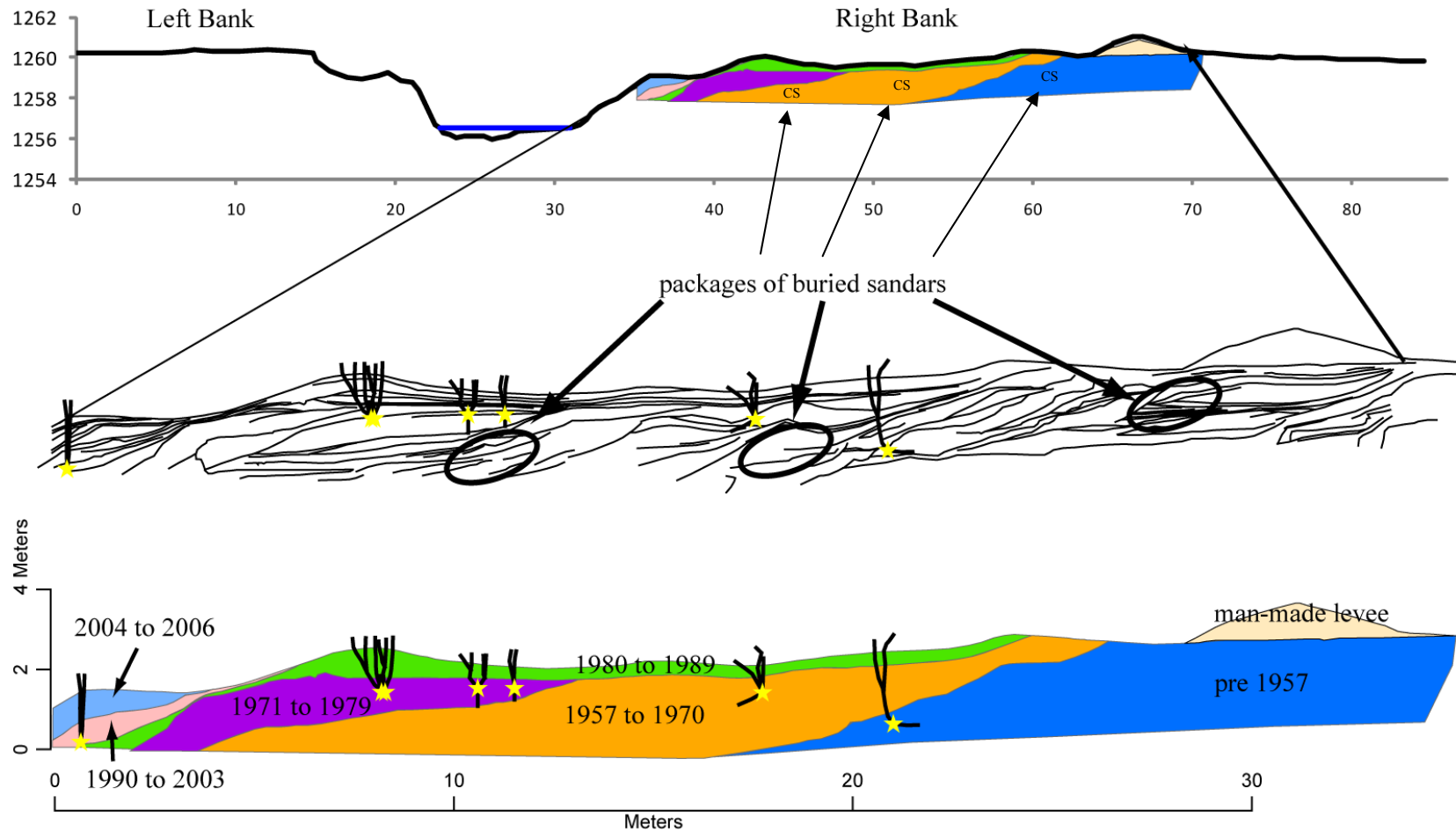


Figure 22. Rating relations constructed for the time period between 1947 and 1976 at original location of the USGS gage. Colors are *not* correlated to the packages of sediment in the Hatt Ranch trench.



**Figure 23. Hatt Ranch floodplain stratigraphy. Successive decrease in the elevation of buried sandbars toward the present day channel indicates that the channel incised and narrowed concurrently. “CS” in the top cross section shows the location of buried sandbars. Yellow stars show the germination locations of Tamarisk trees.**

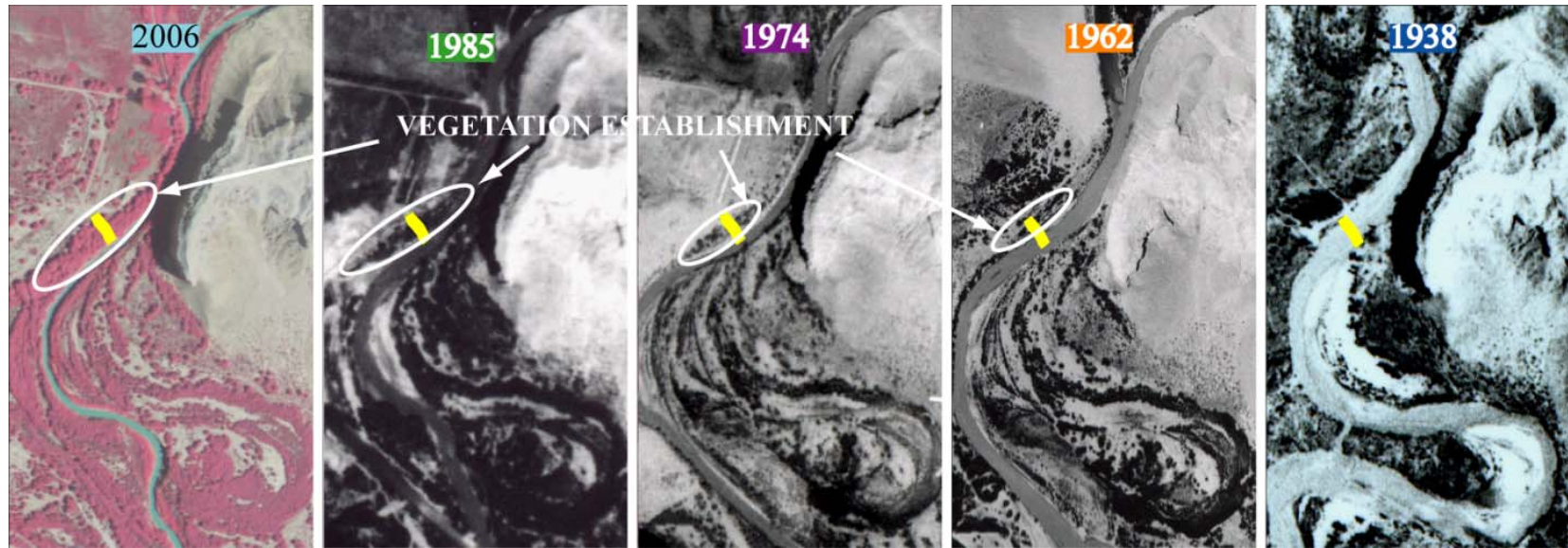


Figure 24. Series of aerial photographs show planform changes in vicinity of Hatt Ranch trench. Trench is indicated by a yellow polygon. Colors behind year titles correlate to colors of sedimentary packages in figure 13.

Table 7. Relevant information for the eight series of aerial photographs analyzed in this study.

Year	Type	Flight date	Scale	Size	Source	Streamflow (ft <sup>3</sup> /s)	Coverage	Length (km)
1938	B&W prints	July 6 & 20	1:31680	10 x 10 in	NARA archives	unknown	entire lower river	87.3
1952	B&W prints	November 17	1:20000	9 x 9 in	USGS EROS earth explorer website	76	entire lower river	87.3
1962	B&W prints	June 16	1:20000	15 x 15 in	USDA aerial photography field office	791	partial (see map)	59.7
1974	B&W prints	September 26	1:40000	12 x 12 in	USDA aerial photography field office	35	partial (see map)	40.6
1985	B&W prints	August 15	1:60000	17 x 17 in	USDA aerial photography field office	76	entire lower river	87.3
1997	B&W DOQ	July 4 & 14	1 meter	11.00 x 13.97 km	AGRC website	70 and 53	entire lower river	87.3
2006	CIR DOQ	August 26	1 meter	6.12 x 7.61 km	AGRC website	103	entire lower river	87.3
2010	natural color georeferenced files	August 25	~.25 m	unknown	BOR	11	entire lower river	87.3

### *1960s and 1970s*

The hydrology during the 1960s and 1970s was characterized by dampened snowmelt floods and regularly occurring, moderate warm season floods. The mean annual flow decreased 47% from 1910-1918 to 1946-1958, and again decreased 34% from 1946-1958 to 1959-1979 (Table 2). The reduction in the magnitude and duration of the snowmelt flood during the 1960s and 1970s reduced the channel's capacity to accommodate large flows. In addition, the dampened snowmelt floods allowed tamarisk to quickly establish on previously bare, active channel surfaces and grow denser on previously colonized floodplain surfaces. Tamarisk spread quickly throughout the floodplain during this time period, as shown in the 1974 aerial photographs. The effect of a steady supply of fine sediment from warm season floods, vegetation establishment, and reduced snowmelt floods presumably acted together to create a positive feedback, in which the channel quickly transformed into a narrow slot with cohesive banks. During this time period, an entrenched, narrowed channel with tall banks provided much less complex habitat for native fish.

Channel narrowing, in conjunction with vegetation establishment, occurred along the length of the lower river. A qualitative comparison of aerial photographs from 1952, 1962, and 1974 shows an increase in vegetation density during this time span and also a decrease in channel width. In a quantitative evaluation of RAACW, the channel narrowed at a rate of 0.6 m/yr between 1962 and 1974. Also, between 1938 and 1985 sinuosity increased from 1.34 to 1.58. The increase in sinuosity is likely a response of the collective contribution of the driving mechanisms but especially the increase in bank cohesion due to vegetation establishment. At the USGS gage the average "active" channel width decreased 55% between 1945-1953 and 1959-1977.

Not only did the width of the channel shrink but the shape of the channel also changed. During the early 1960s, the channel capacity decreased for the entire range of stream-flows (Figure 25). Thus, the shape of the channel did not change much as it shrunk. In contrast, the channel during the late 1960s and early 1970s transformed into an entirely different shape. The hydraulic geometry relationship for width for the time period 1965-1976 indicates the channel increased for discharges less than approximately 100 ft<sup>3</sup>/s, and decreased for discharges larger than 100 ft<sup>3</sup>/s (Figure 25). In other words, the channel shape transformed in 1965-1976, such that width expanded more slowly for increasing discharges. For example, the slope of the regression line (exponent *b*) decreased from 0.38 in 1958-1965 to 0.23 in 1965-1976. The drastic decrease in the value "b" indicates that the channel transformed into a box with steep vertical banks. Both incision and inset formation worked in concert to create the "U-shaped" channel.

The power law formula for the time period 1965-1976 does not represent the data as well as the power models do for the other time periods. The R value for 1965-1976 is 0.72. In particular, the regression line does not fit the data well for discharges less than approximately 20 ft<sup>3</sup>/s. In other words, the channel seems to accommodate low discharges quite differently than it does higher discharges.

Both an analysis of covariance (ANCOVA) and plotting confidence bands for distinct periods of time for the width hydraulic geometry relationship helped in determining the appropriate time periods of adjustment. Table 11 displays the results from the ANCOVA. Since all of the P values for the paired ANCOVA tests are approximately zero, it can be said that the chosen time periods have a 99.9% probability that their distinctness from each other did not occur by chance. Also, the  $R^2$  results explain the power model's ability to judge the variance in width. Since the range of values of  $R^2$  (.64 to .85) are greater than .6, then there is a strong correlation between the power model and the data of each time period. Furthermore, the F statistic values show that the variances between the power models of adjacent time periods are significantly different. The ANCOVA results and the 95% confidence bands indicate that four time periods 1909-1958, 1958-1965, 1965-1976, and 1976-2005 are statistically significant and therefore do represent actual periods of channel adjustment. In other words, the shape of the relationship between width and discharge changed significantly four times over the course of the period of record.

Sediment-rich, warm season floods contributed sediment to the growth of inset deposits which formed along both banks. An inset deposit, which is defined as the horizontal and vertical accretion of a sandbar within a formerly wide active channel (Allred and Schmidt, 1999; Dean and Schmidt, 2010), formed along the left bank at the abandoned cableway (Figure 21). The formation of an inset deposit on the left bank between 1958 and 1970 effectively narrowed the channel by approximately 50%. And, inset deposition occurred at the floodplain trench approximately 1 kilometer downstream from the abandoned cableway. Thus, it can be assumed that the same style of floodplain construction that occurred on the right bank as revealed in the Hatt Ranch trench was also responsible for the creation of the inset deposit on the left bank further upstream at the abandoned cableway.

Interpretation of floodplain stratigraphy yields insight into the internal character of inset deposits. The internal stratigraphy of two levees on the Hatt Ranch reveals that sand bars that formed on the bed of the river, accumulated sediment until they became stable features of the floodplain. At the base of two natural levees, channel margin sand bars (denoted in Figure 23 as "CS") are comprised of cross-stratified sand and lenses of mud. Overlying the sand bars are mud-capped packages of silty-sand, which transition into thick packages of cross stratified, silty sand at the crests of the levees.

Dendrogeomorphic results indicate that vegetation played an important role in stabilizing sand bars and facilitating both lateral and vertical accretion. Previous studies have speculated that tamarisk and other riparian vegetation facilitate the deposition of sediment by increasing the threshold of erosion by stabilizing an unconsolidated fluvial surface (Dietz, 1952; Pollen-bankhead et al, 2009), and increasing roughness which in turn slows the water velocity during a flood flow (Griffin et al, 2005). At slower velocities, therefore, suspended sediment decants from

the water and is deposited on the floodplain surface. The preserved packages of former sand bars stepping down in elevation toward the channel indicates that channel incision occurred in conjunction with channel narrowing. Incision and the conversion of sand bars to stable floodplain features have disconnected the floodplain from the main channel, thereby reducing important resources for native fish.

Following a wave of rapid incision in the 1950s, the rate of incision slowed during the early 1960s. Between 1958 and 1965 the elevation of the bed decreased at a rate of approximately 0.05 meter/year for a total decrease of 0.3 m in bed elevation. The snowmelt flood of 1965 temporarily halted incision and initiated a wave of aggradation which continued for 11 years. During the rising stages of the 1965 flood, which behaved similarly to the snowmelt flood 1958, the bed filled approximately 0.6 m. However, unlike the snowmelt flood of 1958, three monsoon floods occurred during the flood's recession, prevented the bed from scouring to the pre-flood elevation, and consequently a net increase in bed elevation of approximately 0.3 m occurred.

In contrast to the geomorphic effect of the snowmelt floods of the 1950's, the meager snowmelt floods of the late 1960's and 1970's facilitated bed filling. In fact, there is no evidence of scouring during the peaks of the late 1960s and 1970s snowmelt floods, rather the bed responded to the increase in flood stages, by filling. During the falling limb of the hydrograph of each of these floods, the bed either returned to its antecedent elevation, or failed to scour to the bed level prior to the flood, resulting in a net increase in bed elevation. As a result, between 1965 and 1976, the bed slowly filled at a rate of 0.03 m/yr for a total bed increase of approximately 0.5 m. Also, during the 1960s and 1970s the rating relations steepened at higher discharges (Figure 22). Steepening of the relations indicate that the channel narrowed. The reduction in cross section area, in combination with bed lowering, resulted in a confined channel where moderate discharges, now achieved a higher stage. The reduction in channel capacity allowed smaller floods than previous to spill over the channel's banks and thus contribute to additional floodplain aggradation.

Modifications to both the channel and the floodplain have influenced the behavior of the channel and floodplain formation on the Hatt Ranch. The Hatts constructed levees in the 1970s to prevent the river from flooding their property. In addition, the Hatts straightened the channel by filling the channel in two places, thereby cutting off two meander bends. Also, construction of two bridges for Highway 24 likely constricted the natural migration of the river. The construction of the diversion dam prior to the 1950s as well as the establishment of vegetation may have contributed to the incision of the channel, however this is highly speculative. Furthermore, channel straightening may have facilitated incision but was not the initial cause, because we know that the 1952 snowmelt flood initiated incision. The following excerpt from the 1962 USGS station analysis report of 1962 describes the channel straightening on the Hatt Ranch:

*“During the period Nov 30 (1961) to May 15(1962) the owner of the land in the vicinity of the gage straightened the channel downstream from the gage by removing two large oxbows. This was accomplished by excavating a shallow channel across the gooseneck of one oxbow, then throwing a dike across the main channel just below it, and allowing the flow to erode the new channel down to grade. This was repeated on the second oxbow, the main channel being diked off on March 21. This caused the channel to scour down lower than it had ever been before, and made lowering of the gage necessary. Backwater at the gage caused by these operations resulted in some very large shifting-control adjustments during the period mentioned.”*

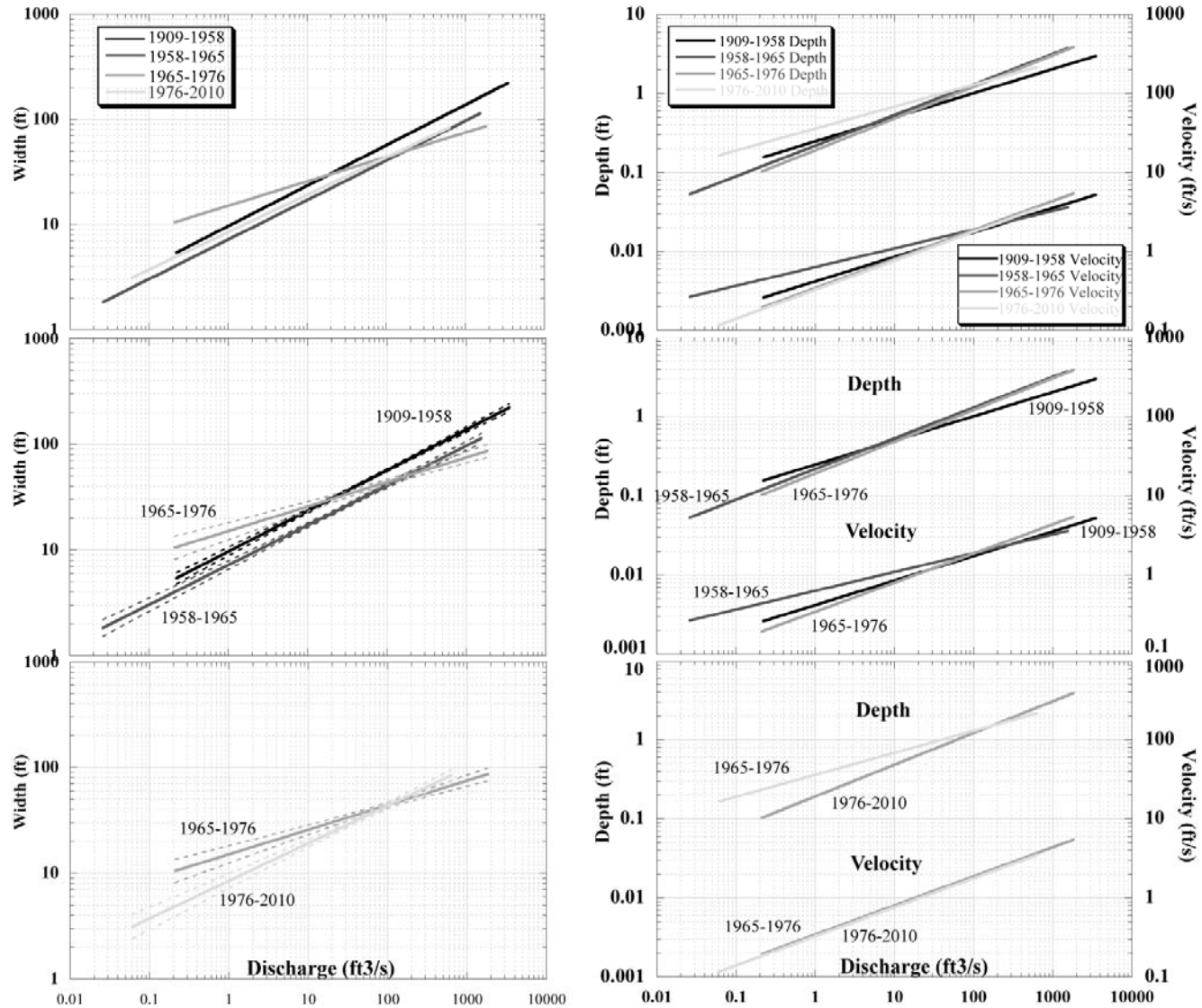


Figure 25. Hydraulic geometry relationships for width, depth and velocity at the USGS gage 09328500. Note units are in English and 1 ft = 0.3048 m.

**Table 8. Components of the width hydraulic geometry relationship formula ( $w=aQ^b$ ) and the value for the Pearson's product moment correlation coefficient (R).**

Time period	Equation	Exponent b	Coefficient a	R	Degrees of Freedom (N-2)	Adjusted R <sup>2</sup>	P value
1909-1958	$9.6614 * X^{.38447}$	.38447	9.6614	.87367	395	.8466	2.2E-16
1958-1965	$7.2023 * X^{.37563}$	.37563	7.2023	.85997	264	.8376	2.2E-16
1965-1976	$15.097 * X^{.23197}$	.23197	15.097	.71545	111	.6365	2.2E-16
1976-2010	$8.4685 * X^{.3556}$	.3556	8.4685	.92086	82	.6659	2.2E-16

**Table 9. Components of the velocity hydraulic geometry relationship formula ( $v=kQ^m$ ) and the value for the Pearson's product moment correlation coefficient (R).**

Time period	Equation	Exponent m	Coefficient k	R
1909-1958	$.41795 * X^{.30984}$	.30984	.41795	.9278
1958-1965	$.63416 * X^{.23701}$	.23701	.63416	.89441
1965-1976	$.34451 * X^{.36765}$	.36765	.34451	.97472
1976-2010	$.32716 * X^{.36695}$	.36695	.32716	.94293

**Table 10. Components of the depth hydraulic geometry relationship formula ( $d=cQ^f$ ) and the value for the Pearson's product moment correlation coefficient (R).**

Time period	Equation	Exponent f	Coefficient c	R
1909-1958	$.24804 * X^{.43335}$	.30539	.24804	.72275
1958-1965	$.21881 * X^{.38628}$	.38748	.21881	.95322
1965-1976	$.19195 * X^{.38954}$	.40069	.19195	.96916
1976-2010	$.3605 * X^{.3632}$	.27769	.3605	.91433

**Table 11. ANCOVA results for paired time periods shows that each chosen time period is significantly different from the next time period.**

Paired time periods	Adjusted R <sup>2</sup>	F-statistic	P value
1909-1958 to 1958-1965	.8707	1487	2.2E-16
1958-1965 to 1965-1976	.8319	624.7	2.2E-16
1965-1976 to 1976-2005	.6749	152.6	2.2E-16

### 1980s

The trend of declining streamflow reversed in the 1980s when the volume of snowmelt floods, and thus total flow, increased. The mean annual flow for the time period 1980-1986 (255 ft<sup>3</sup>/s) increased 2.8 times from the previous time period. Two extremely large snowmelt floods occurred in 1983 and 1984; they contained the largest and second largest runoff volumes of the

entire pool of snowmelt floods (Table 1), yet the third and sixth largest flood peaks of all snowmelt floods. The snowmelt floods of 1983 and 1984 widened the channel in places, caused vertical accretion of the established floodplain, and lowered the elevation of the bed on the Hatt Ranch. During the same period in the 1980s, warm season floods contributed to both channel narrowing and vertical accretion of the floodplain.

Channel widening occurred sometime prior to 1985, most likely during the snowmelt floods of 1983 and 1984. Portions of the floodplain were destroyed and point bars were created in the wake of the erosion, as seen in aerial photographs taken in 1985 (Figure 17). The floodplain destruction resulted in an increase in the average width of the “active channel” during the time period, 1976-1986 (Figure 14). The temporary increase in channel width was spatially extensive; the RAACW increased 15% from 1974 to 1985. Furthermore, where the snowmelt floods in 1983 and 1984 weren’t able to completely destroy the floodplain they were still able to strip sediment from the floodplain and add new layers of sediment (green colored package of sediment in Figure 23). The package of sediment denoted in green in Figure 23 comprise the upper most portion of the levee closest to the modern channel and part of the more distal levee.

The snowmelt flood of 1983 initiated a wave of incision at the current location of the USGS gage. A short time period prior to the onset of the snowmelt flood of 1983, was characterized by neither net aggradation nor degradation, and highlighted by significant scouring during four snowmelt floods between 1980 and 1982. During the falling stages of each flood, the bed filled to the approximate pre-flood elevation. Then, the snowmelt flood of 1983 lowered the bed 2 ft. Since discharge was not measured during the peak of the 1983 flood, the full extent of the magnitude of scour at the peak is not known. Following the 1983 snowmelt flood, another large snowmelt flood in 1984 occurred, yet ironically failed to cause a net decrease in bed elevation. The remainder of the 1980s was characterized by no changes in bed elevation.

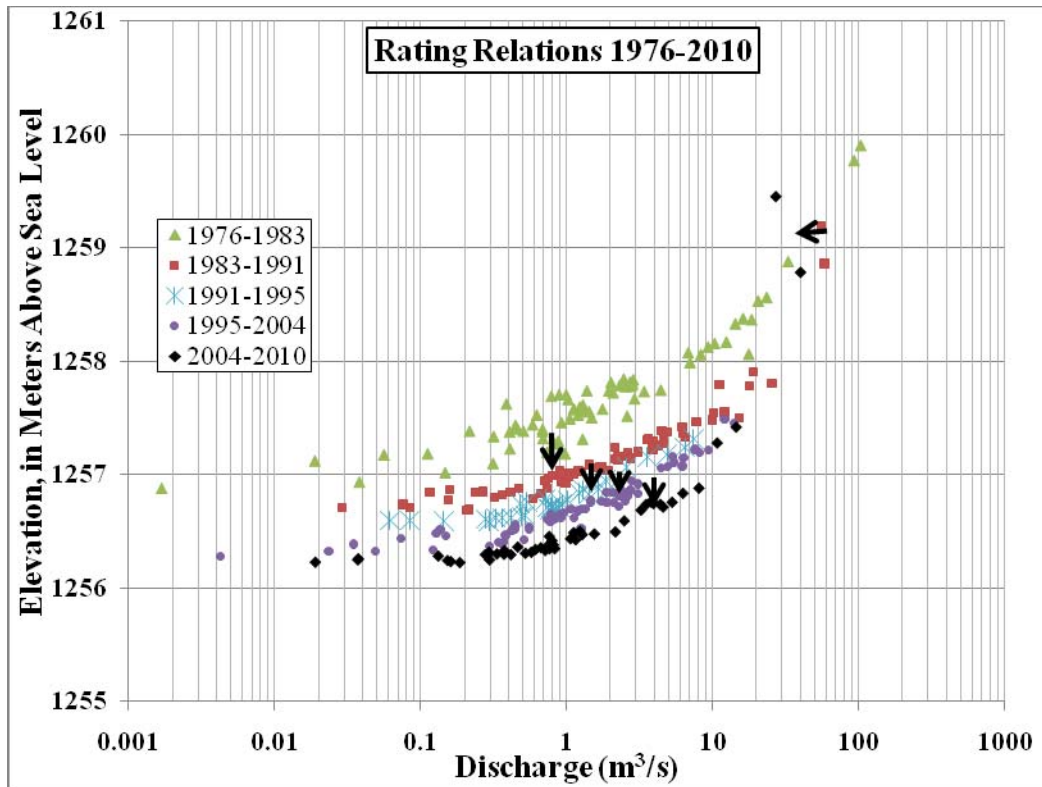


Figure 26. Rating relations constructed for the time period between 1976 and 2008 at the current location of the USGS gage.

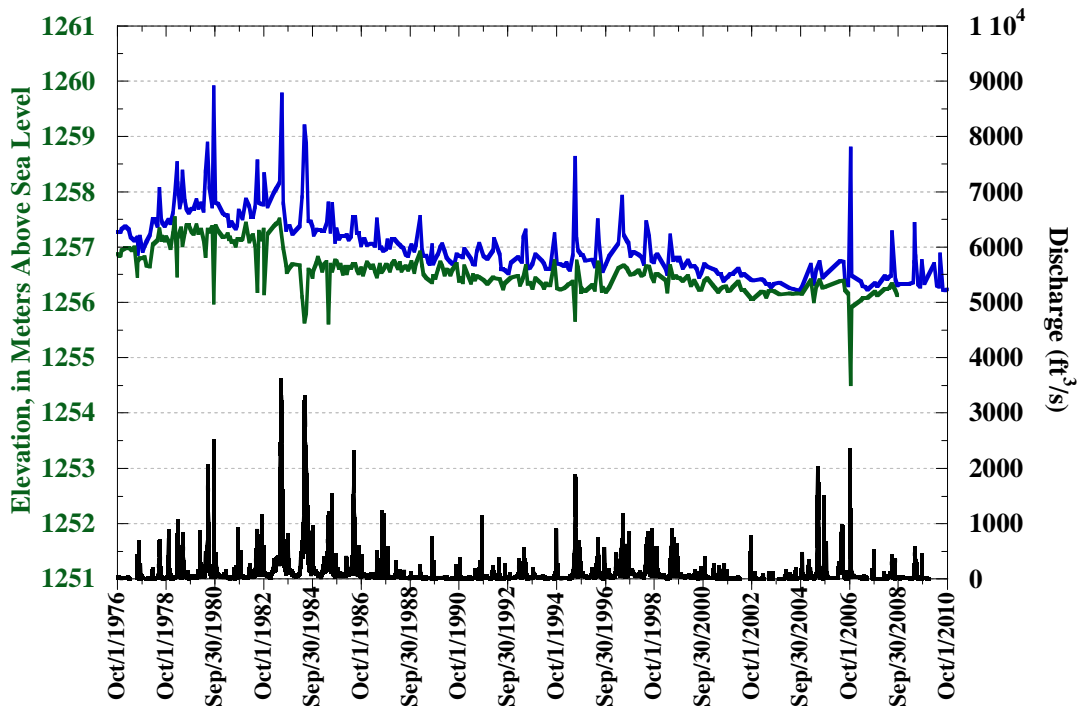


Figure 27. Time series of MINSBE, water surface elevation and discharge between 1976 and 2008.

### *1990s to present*

The channel-floodplain system of the San Rafael River continued in the trajectory of change during the most recent two decades. The channel continued to narrow and incise, and new floodplain deposits have been constructed. Consequently, the channel's capacity to contain large floods has decreased. The hydrology of the last two decades responsible for geomorphic change consisted of dampened snowmelt floods and persistent, moderate warm season floods. The mean annual flow for the period 1987-2010 was 67.2 ft<sup>3</sup>/s, which was approximately 50% smaller than the mean annual flow for the entire period of record, 131.2 ft<sup>3</sup>/s. In contrast to the 1980s, when five of the seven years between 1980 and 1986 experienced snowmelt floods that exceeded 1000 ft<sup>3</sup>/s, only two snowmelt floods during the most recent two decades achieved a peak greater than 1000 ft<sup>3</sup>/s. The peak of the snowmelt flood of 1997 was 1170 ft<sup>3</sup>/s and the peak of the snowmelt flood of 2005 was 2010 ft<sup>3</sup>/s. Interestingly, during the last two decades, a period characterized by meager snowmelt floods, the bed scoured by approximately 1 foot.

An overall trend of bed lowering between 1990 and 2010 was interrupted by one discrete, aggradational event. Between 1990 and 1997, the bed lowered approximately one foot. Then, the snowmelt flood of 1997 filled the bed approximately 1 foot. Since 1997, the bed has scoured by an additional 1 foot. Further evidence of incision is apparent in the reconstructed cross sections at the abandoned USGS cableway. In August 2009, we measured the cross section at the abandoned USGS cableway, located about 150 m downstream from the old highway 24 bridge. Between 1970 and 2009 the channel incised approximately 2.1 m and narrowed slightly.

Since the 1980s the channel has resumed a trajectory of narrowing, in conjunction with incision. Warm season floods, facilitated by vegetation establishment, deposited fine sediment within the active channel and further confined the San Rafael River. A nearly flat-topped bench exposed at the Hatt Ranch trench is comprised of new sediment accumulated between 1990 and 2006, which overlies sediment deposited in the 1980's (Figure 23). The "near channel bench" observed in the Hatt Ranch trench is a common floodplain feature along much of the length of the lower river and accumulated a brand new layer of mud during the October 2010 flood.

Despite the steady decrease in channel width, recently, channel narrowing has occurred at a slower rate than the 1960s and 1970s, because accommodation space has been considerably less. Space available for narrowing in the 1950s was not available in the most recent two decades, despite additional space created by the large snowmelt floods of 1983 and 1984. The RAACW decreased by approximately half between 1985 and 2006, however the rate of narrowing was slower for the most recent period (1985-2006) than for the first period, 1 m/yr and 0.6m/yr, respectively. Average "active" channel width at the USGS gage was 13.7 m for the most recent period (1987-2010), which is a 59% decline from the time period that exhibited the greatest mean channel width, 1945-1953.

The shape of the channel since 1976 resembled the channel shape during the time period 1958-1965, prior to the “box shape” transformation. The slope of the regression line for the time period 1976-2010 is similar to the regression line slope for the time period 1958-1965, which means the width of the channel accommodated discharge in a similar fashion to the period of 1958-1965. The return in channel shape to that of the early 1960’s is perplexing and warrants speculation into the possible causes. In 1983 and 1984, large snowmelt floods widened the channel in places, and perhaps a portion of the channel close to the gage eroded. Or, the hydraulic geometry relationships of 1965-1976 and 1976-2005 may differ because the gage was moved downstream in 1976 approximately 1.6 km; however it is assumed that the shape of the channel is not fundamentally different over this distance because no tributaries or significant geomorphic agents that may alter the shape of the channel occur between these two gage locations. Despite the confounding evidence in the hydraulic geometry relationship for width, the rating relations indicate that the combination of incision and channel narrowing has created a narrow slot with tall vertical banks. Since 1976, the stage discharge relation at higher discharges steepened, which indicate a reduction in channel capacity. Furthermore, the combination of the reduction in the mean annual flood, the reduction in channel capacity, and further vegetation establishment continues to result in overbank flooding and vertical accretion, and channel narrowing.

#### *Longitudinal Profile*

Observation that the river is on bedrock demonstrates that the pattern of incision, observed on the Hatt Ranch, extends along the length of the river. In addition, the bedrock bed is also preventing further incision. In Figure 28, it is apparent that the shape of the water surface profile is nearly straight, and even slightly convex between the Hatt Ranch diversion dam and the confluence with the Green River. We will address the potential reasons for the observed shape of the San Rafael River in Fortney’s master thesis.

Hydraulic controls over the length of the longitudinal profile consist of beaver dams, tributary confluences, and bedrock. The overall water surface slope of the lower river is 0.001. Except for the short reach downstream from the diversion dam, the slopes for the various reaches diverge less than .0003 from the overall slope. Where tributaries enter the mainstem, we observed pools upstream from the confluences and steeper gradient riffles comprised of coarser material, downstream from the confluence. Figure 29 is a longitudinal profile in the vicinity of the confluence with Iron Wash, upstream from Frenchman’s Ranch. Two beaver dams within 1 km upstream from Iron Wash create a stair-stepped profile. A steep gradient consisting of gravel riffles occurs downstream from Iron Wash for approximately .5 km. A similar sequence of geomorphic units occurs where the river is on bedrock. Figure 30 is the longitudinal profile of the most downstream reach of the San Rafael River. Two beaver dams occur less than 1 km upstream from a bedrock knickpoint. A steeper reach comprised of gravel riffles extends for approximately .2 km downstream from the bedrock knickpoint.

**Table 12. Water surface slopes for selected reaches in the lower San Rafael River. Longitudinal profile data was used to calculate these slopes.**

<b>reach</b>	<b>slope</b>	<b>elevation loss (m)</b>	<b>distance (m)</b>	<b>distance (km)</b>
entire lower river	0.0010	87.3	85146.6	85.1
Reef to Hatt Ranch diversion dam	0.0008	16.3	21536.2	21.5
diversion dam	0.0325	5.6	171.1	0.2
diversion dam to upstream end of confined alluvial valley reach	0.0010	31.8	33421.5	33.4
confined alluvial valley reach	0.0011	28.3	25717.2	25.7
downstream end of alluvial valley reach to the confluence	0.0012	5.3	4300.6	4.3

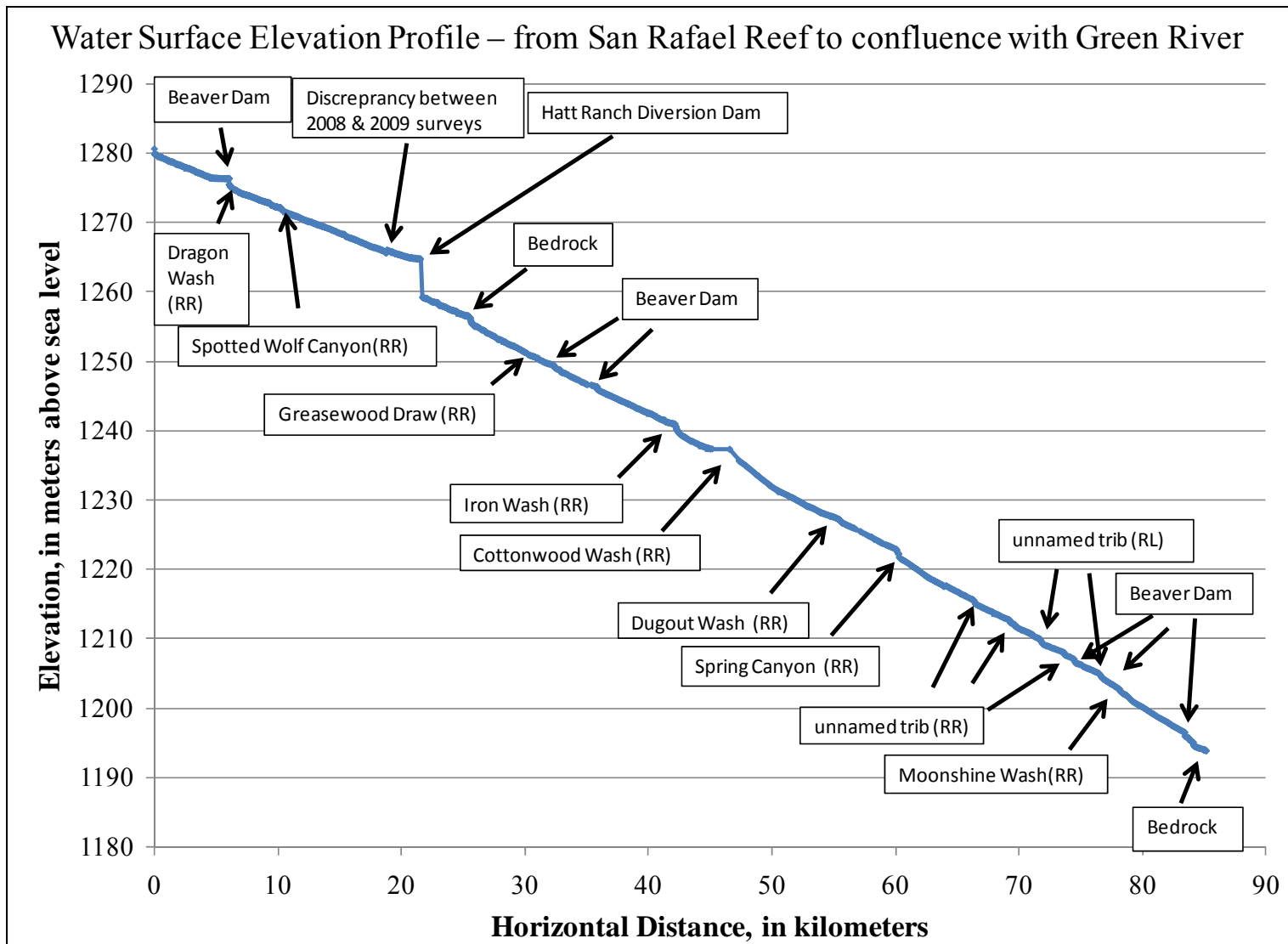


**Figure 28. Longitudinal profile of water surface and bed elevations for entire length of the lower San Rafael River, between the San Rafael Reef and the confluence with the Green River.**

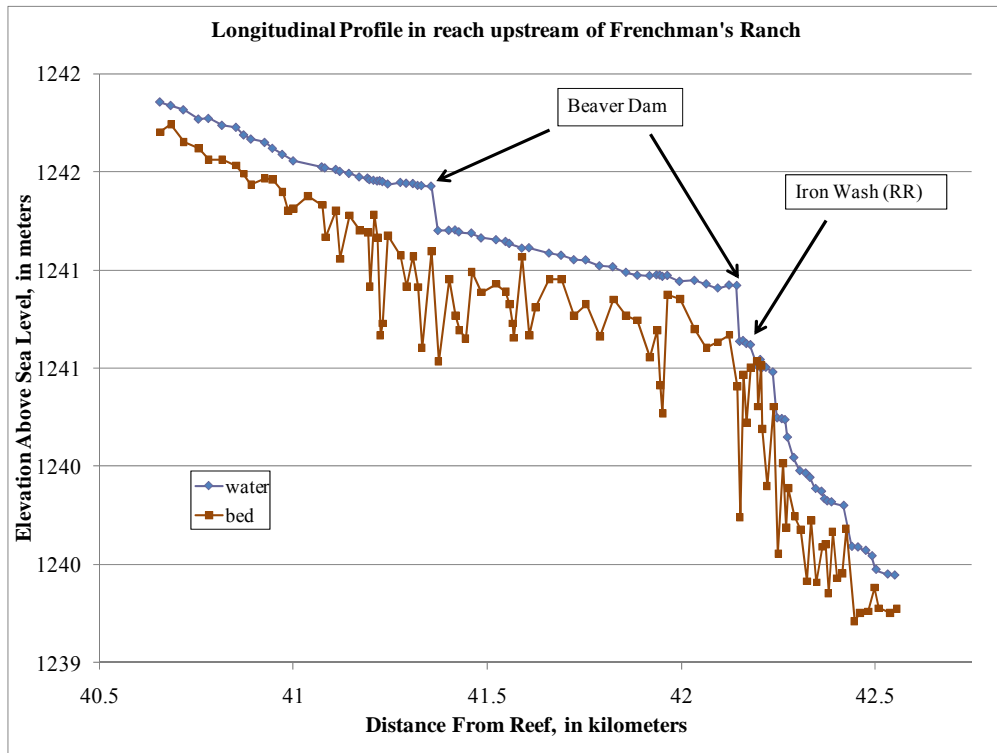


**Figure 29. Longitudinal profile of the water surface and bed elevations for a 2.25 kilometer reach upstream of Frenchman’s Ranch**

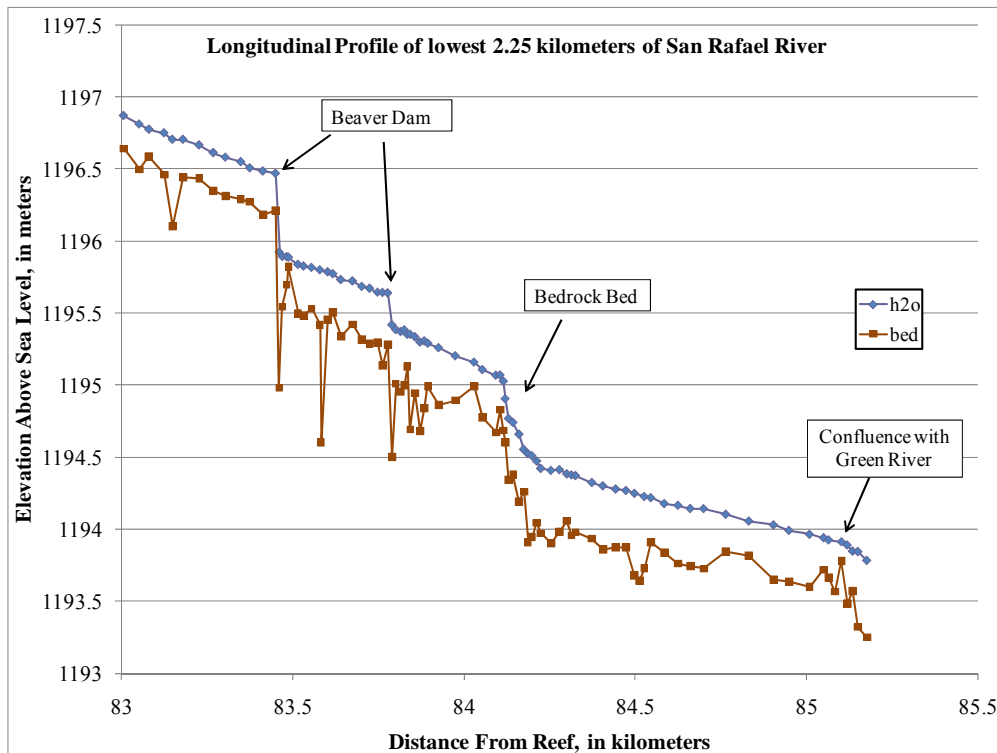


**Figure 30. Longitudinal profile of the water surface and bed elevations for the lowest 2.25 kilometer reach of the San Rafael River, before the confluence with the Green River.**

## **VII. Summary**

### ***A. Channel Transformation on Hatt Ranch***

Streamflow has declined in the San Rafael River over the last 100 years. Extensive diversions for energy development and agriculture in the headwaters have drastically reduced the duration and magnitude of the snowmelt flood such that the median annual snowmelt flood for the most recent decade is 93% shorter in duration and the peak is 67% smaller than the snowmelt flood of the second decade of the 1900s. Furthermore, the mean annual flow declined 75% from the first time period 1909-1920 to the most recent time period 1987-2010, with the exception of the period 1980-1986, which caused a temporary increase in the mean annual flow. The magnitude of the warm season floods have also decreased since the 1950s, however their frequency does not seem to have changed. Historically, the hydrograph was dominated by snowmelt floods and currently the annual hydrograph is dominated by warm season floods. The shift in the relative importance of the two peaks in the annual hydrograph has contributed to significant geomorphic change in the San Rafael River, thereby limiting the complexity of fish habitat and connection between the channel and floodplain.

Reduction of the of the snowmelt flood in both magnitude and duration has allowed Tamarisk to colonize both active channel bars and floodplain surfaces. The establishment of Tamarisk and other riparian vegetation species, such as willow and grasses, has facilitated the conversion of active channel surfaces to floodplain surfaces by inducing sedimentation during sediment-rich warm season floods. Collectively, a reduced snowmelt flood, fine sediment deposition during warm season floods, and tamarisk establishment has drastically narrowed the San Rafael River. Narrowing began in 1953 and has been accomplished by the vertical and lateral accretion of inset deposits. High rates of inset deposition occurred between 1957 and 1979. The amount of active channel surfaces has decreased 77% between 1938 and 2006. Furthermore, steepening of the rating relations indicates a reduction in channel capacity since the early 1960's. Finally, despite a decrease in the rate of channel narrowing since 1990, channel width continues to decrease.

The San Rafael River is system with an excess of fine sediment as well as a lack of water. This scenario would lead one to expect the style of bed adjustment would be aggradation, not incision, if any bed adjustment were to occur. However, results from four different analyses (rating relations, reconstructed historical cross sections, floodplain stratigraphy, and repeat oblique ground photos) indicate that incision has been occurring in the San Rafael since the 1950's. Two large snowmelt floods (1952 and 1983) initiated two separate waves of incision. Additional smaller snowmelt floods in 1953 and 1957 also resulted in bed lowering. Furthermore, incision occurred during periods without floods, such as in 1953/1954 and 1957/1958. In total, the bed lowered approximately 3.5 m between 1952 and 2009. A survey of the water surface elevation along the length of the lower river shows that the river has eroded to bedrock at three places which demonstrates that the pattern of incision extends all the way to the confluence. In fact, bedrock is limiting further incision in these locations. A lack of precise information concerning the style and magnitude of changes in sediment supply and the timing and extent of vegetation

establishment leading up the 1952 snowmelt flood prevents us from knowing the exact causes of the initiation of incision. However, the available data presented in this report provides a starting point to better understand the timing and magnitude of incision.

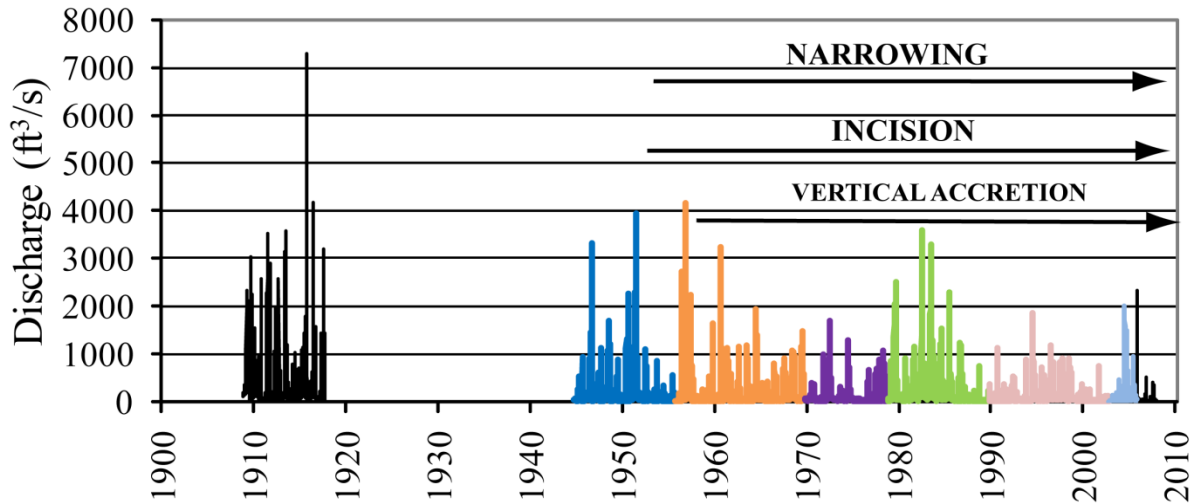


**Figure 31. Hydrograph of the mean daily discharge for the period of record. Colors correlate to sedimentary packages in Hatt Ranch trench, figure 23. The style of channel change is indicated by arrows.**

***B. Restoration and Management Implications***

Restoration of the channel and floodplain of the San Rafael requires a sound scientific understanding of the geomorphic history of the river. For this reason, we hope results from our study will guide the restoration community in developing an effective native fish habitat rehabilitation plan for the San Rafael River. The effort to increase complex fish habitat by removing non-native tamarisk from the riparian zone will be most effective if conducted in sync with the restoration of the snowmelt flood regime (Stromberg et al, 2007). Furthermore, in the 1980s when tamarisk had already been widely established and before efforts to remove the non-native shrub had occurred, the two biggest snowmelt floods in recorded history (1983, and 1984) only temporarily halted channel narrowing. Therefore, it is critical that future rehabilitation efforts address both the need for more water and the mitigation of further tamarisk establishment. Finally, reconnecting the channel to the floodplain for the benefit of the endemic fish species will require addressing the incision of the San Rafael River.

## VIII. Expenditures

Table 13 provides an accounting of project money spent through December 31, 2010. These expenditures include the costs associated with the activities described above as well as money spent for a monthly graduate student stipend, salaries, benefits, travel, and other indirect costs. The contract ends on December 31, 2010, therefore remaining work is authorized to be completed at a no cost extension.

**Table 13. USU final invoice for reimbursement of expenditures for the Cooperative Agreement Number #68-3A75-4-155. Also shown is the total amount allocated for individual categories in the contract.**

	Current	Cummulative
Salary & Wages	\$ 16,613.01	\$ 65,775.80
Benefits	\$ 5,531.61	\$ 14,115.29
Travel	\$ 784.45	\$ 3,538.72
Current Expenses	\$ 248.31	\$ 12,369.51
Indirect Cost	\$ 2,317.57	\$ 9,200.68
<b>Total</b>	<b>\$ 25,494.95</b>	<b>\$ 105,000.00</b>

## IX. Timeline

**Table 14. Timeline of remaining activities to be completed by the end of the project.**

Season	Activity
<i>2011 Spring</i>	<ul style="list-style-type: none"> <li>– georeference 1938 and recently acquired 1952 aerial photographs</li> <li>– complete analysis of aerial photographs in GIS</li> <li>– complete dendrogeomorphic analysis of floodplain deposits at Frenchmans Ranch</li> <li>– sample bed material in lower river</li> <li>– complete surficial geologic map of alluvial valley</li> <li>– acquire remaining oblique photos and match them to current photos</li> </ul>
<i>2011 Summer</i>	– write thesis and produce final report
<i>2011 Fall</i>	– defend thesis

## X. References

Alexander, J.S., Zelt, R.B., Schaepe, N.J. 2009. Geomorphic Segmentation, Hydraulic Geometry, and Hydraulic Microhabitats of the Niobrara River, Nebraska – Methods and Initial Results. USGS Scientific Investigations Report 2009-5008. 62 p.

Allred, T.M., and Schmidt, J.C., 1999. Channel narrowing by vertical accretion along the Green River near Green River, Utah. Geological Society of America Bulletin 111 (12), 1757–1772.

- Brock, J.H. 1994. *Tamarix* spp. (Salt Cedar), an Invasive Exotic Woody Plant in Arid and Semi-arid Riparian Habitats of Western USA. In: de Waal LC, Child LE, Wade PM and Brock JH (eds) *Ecology and Management of Invasive Riverside Plants*, pp 27–44. John Wiley, West Sussex, UK
- Birken, A.S., and Cooper, D.J., 2006. Processes of tamarix invasion and floodplain development along the lower green river, Utah. *Ecological Applications* 16 (3), 1103–1120.
- Budy, P., T. Walsworth, and G.P. Thiede. 2010. Habitat needs, movement patterns, and vital rates of endemic Utah fishes in a tributary to the Green River, Utah. 2009 Annual Report to the Bureau of Reclamation, Upper Colorado Region. UTCFWRU 2010(1):1-45.
- Dietz, R.A., 1952. The evolution of a gravel bar. *Annals of Missouri Botanical Garden* 39,249-254.
- Dean, D.J., and Schmidt, J.C., 2011. The role of feedback mechanisms in historic channel changes of the lower Rio Grande in the Big Bend region, *Geomorphology* 126 (3-4), 333-349.
- Dunne, T., and Leopold, L.B., 1978. *Water in Environmental Planning*. San Francisco: W.H. Freeman.
- Friedman, J.M., Vincent, K.R., Shafroth, P.B., 2005. Dating floodplain sediments using tree-ring response to burial. *Earth Surface Processes and Landforms* 30 (9), 1077–1091.
- Geary, E. A, 1996. *A History of Emery County*. Utah Centennial County History Series. Salt Lake City: Utah State Historical Society. 448 p.
- Graf, W.L., 1978. Fluvial adjustments to the spread of tamarisk in the Colorado Plateau region. *Geological Society of America Bulletin* 89, 1491–1501
- Hereford, R., Webb, R.H., Graham, S., 2002. Precipitation history of the Colorado Plateau region, 1900–2000, US Geological Survey Fact Sheet 119-02 2002. 4 p.
- Kondolf, G.M. and Larson, M. 1995. ‘Historical channel analysis and its application to riparian and aquatic habitat restoration’, *Aquatic Conservation: Marine and Freshwater Ecosystem*, 5, 109–126.
- Leopold, L.B., and Maddock, T., Jr., 1953, *The hydraulic geometry of stream channels and some physiographic implications*: U.S. Geological Survey Professional Paper 252, 57 p.

Pollen-Bankhead, N., Simon, A., Jaeger, K., Wohl, E., 2009. Destabilization of stream banks by removal of invasive species in Canyon de Chelly National Monument, Arizona. *Geomorphology* 103 (3), 363–374.

Rantz, S.E., and others, 1982, Measurement and computation of streamflow: U.S. Geological Survey Water Supply Paper 2175, v. 1, 284 p.

Robinson, T.W. (1965). Introduction, Spread, and Areal Extent of Saltcedar Tamarix in the Western States. Geological Survey Professional Paper 491-A.

Smelser, M.G., and Schmidt, J.C., 1998. An assessment methodology for determining historical change in mountain streams. RMRS-GTR-6, U.S. Department of Agriculture, Forest Service, Rocky Mountain Research Station, Fort Collins, CO. 29 pp.

Stromberg, J.C., Beauchamp, V.B., Dixon, M.D., Lite, S.J., Paradzick, C. 2007. Importance of low-flow and high-flow characteristics to restoration of riparian vegetation along rivers in arid southwestern United States. *Freshwater Biology* 52: 651–679.

Webb, R.H., and Betancourt, J.L., 1992. Climatic variability and flood frequency of the Santa Cruz River, Pima County, AZ, US Geological Survey Water-Supply Paper 2379 1992. 40 p.

Webb, R.H., and J.L. Betancourt. 1990. Climate effects on flood frequency: an example from southern Arizona. In *Proceedings of the Sixth Annual Pacific Climate Workshop*, March 5-8, 1989: California Department of Water Resources, Interagency Ecological Studies Program Technical Report 23, editors: J.L. Betancourt and A.M. MacKay, 61-66.

## XI. Appendix

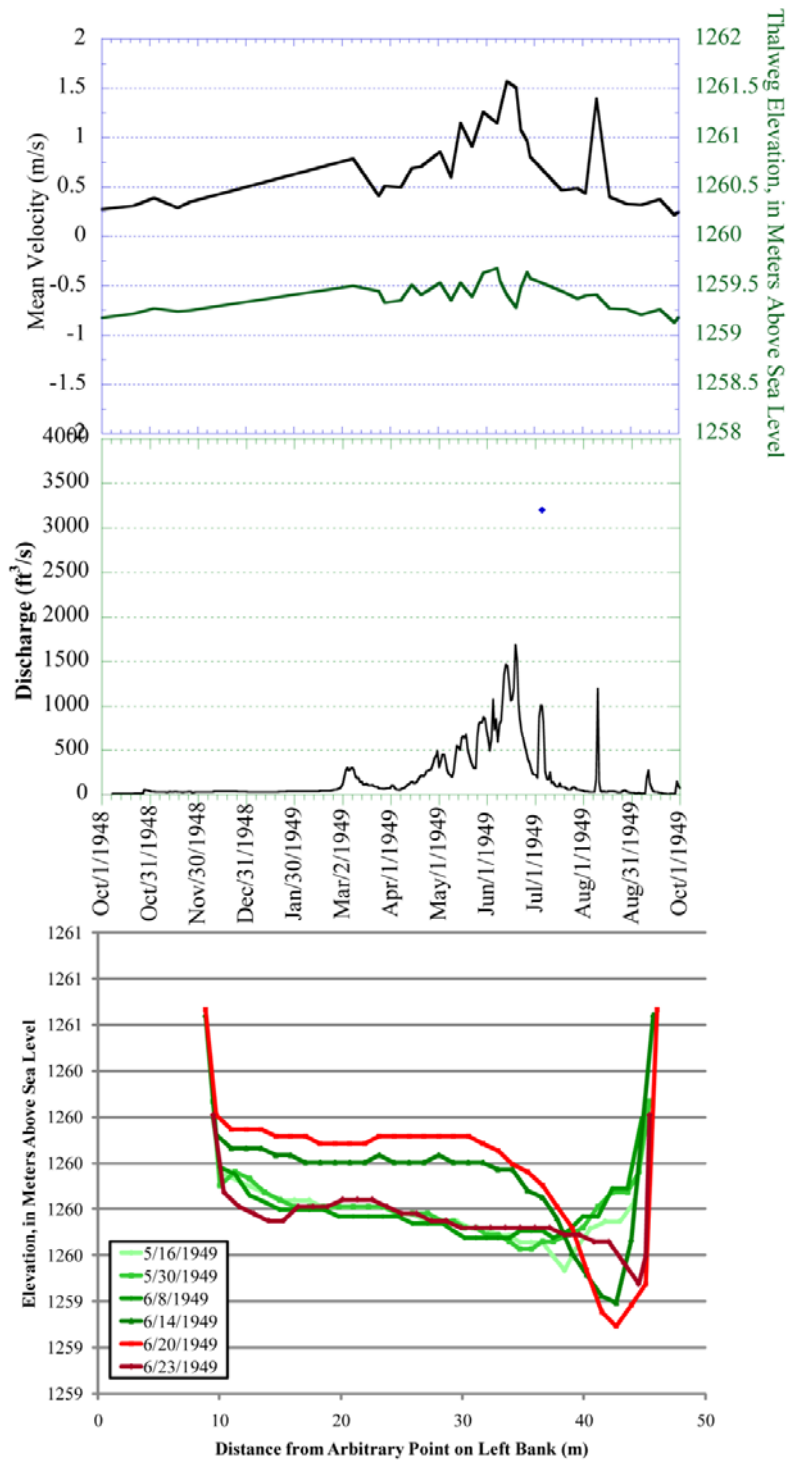


**Figure 32. Cross sections and time series of discharge, MINSBE and velocity during the progress of the snowmelt flood of 1949. Cross sections colored green were measured during the rising limb of the flood hydrograph. Cross sections in red were measured during the falling limb.**

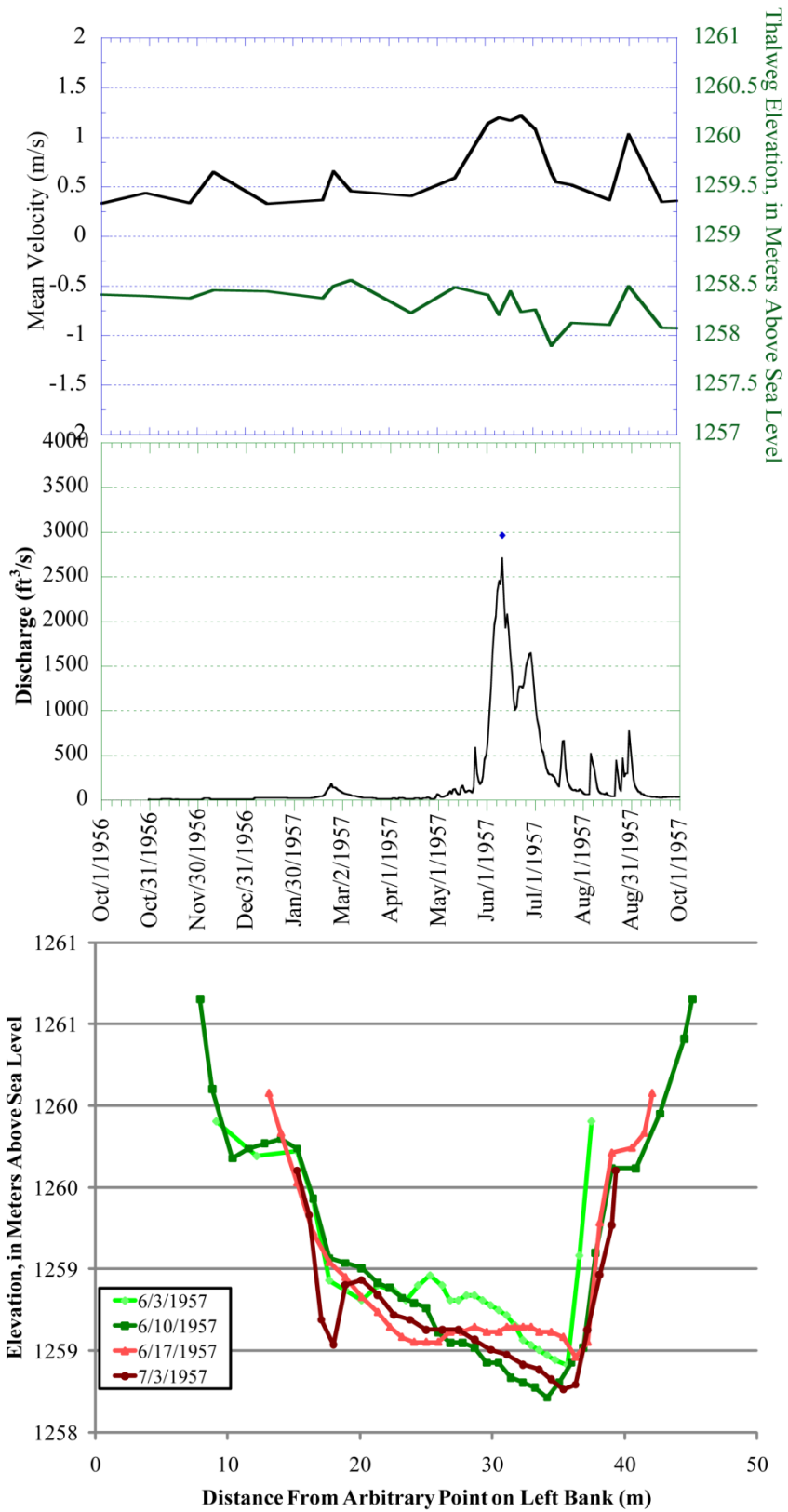


**Figure 33. Cross sections and time series of discharge, MINSBE and velocity during the progress of the snowmelt flood of 1957. Cross sections colored green were measured during the rising limb of the flood hydrograph. Cross sections in red were measured during the falling limb.**

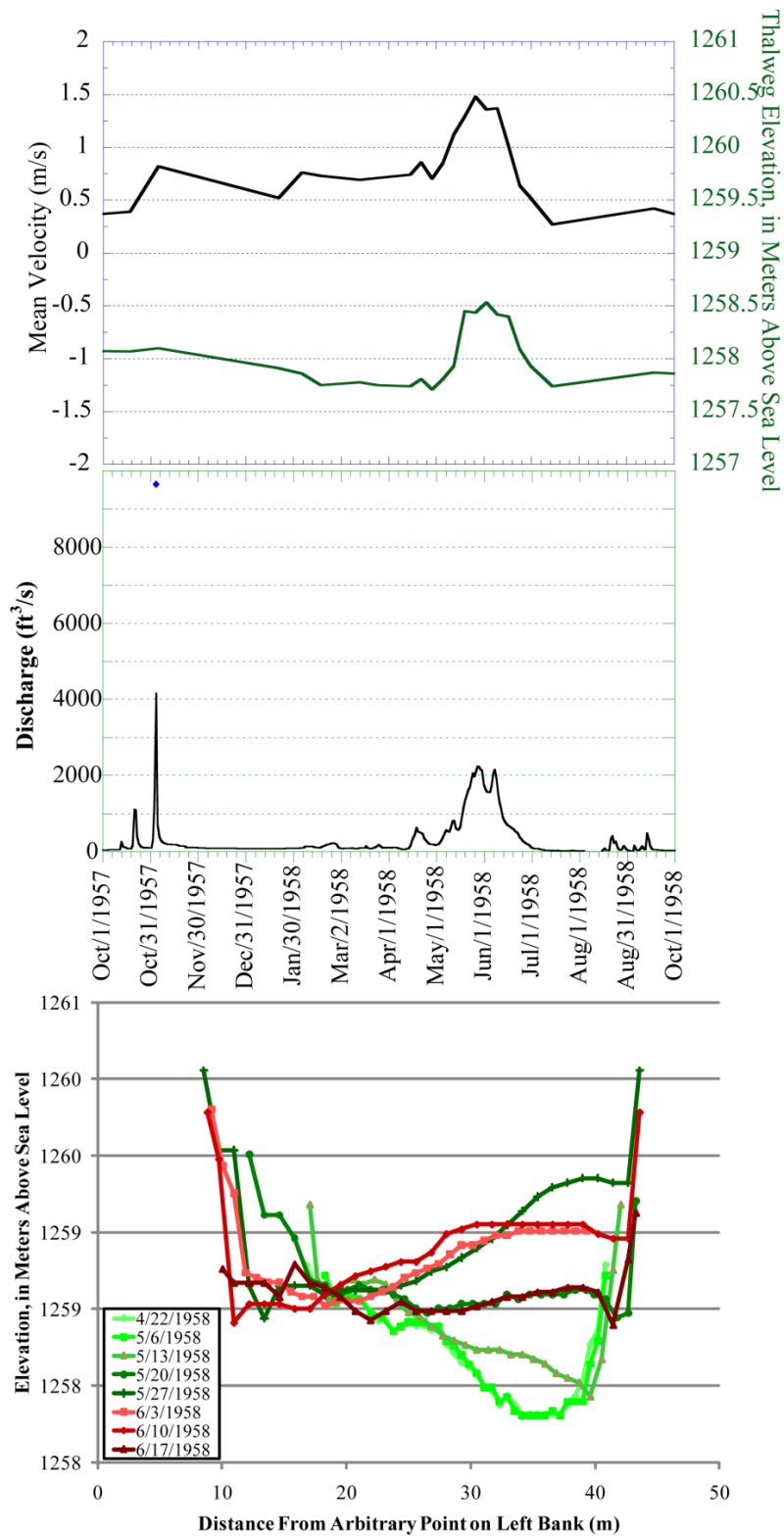


**Figure 34. Cross sections and time series of discharge, MINSBE and velocity during the progress of the snowmelt flood of 1958. Cross sections colored green were measured during the rising limb of the flood hydrograph. Cross sections in red were measured during the falling limb.**

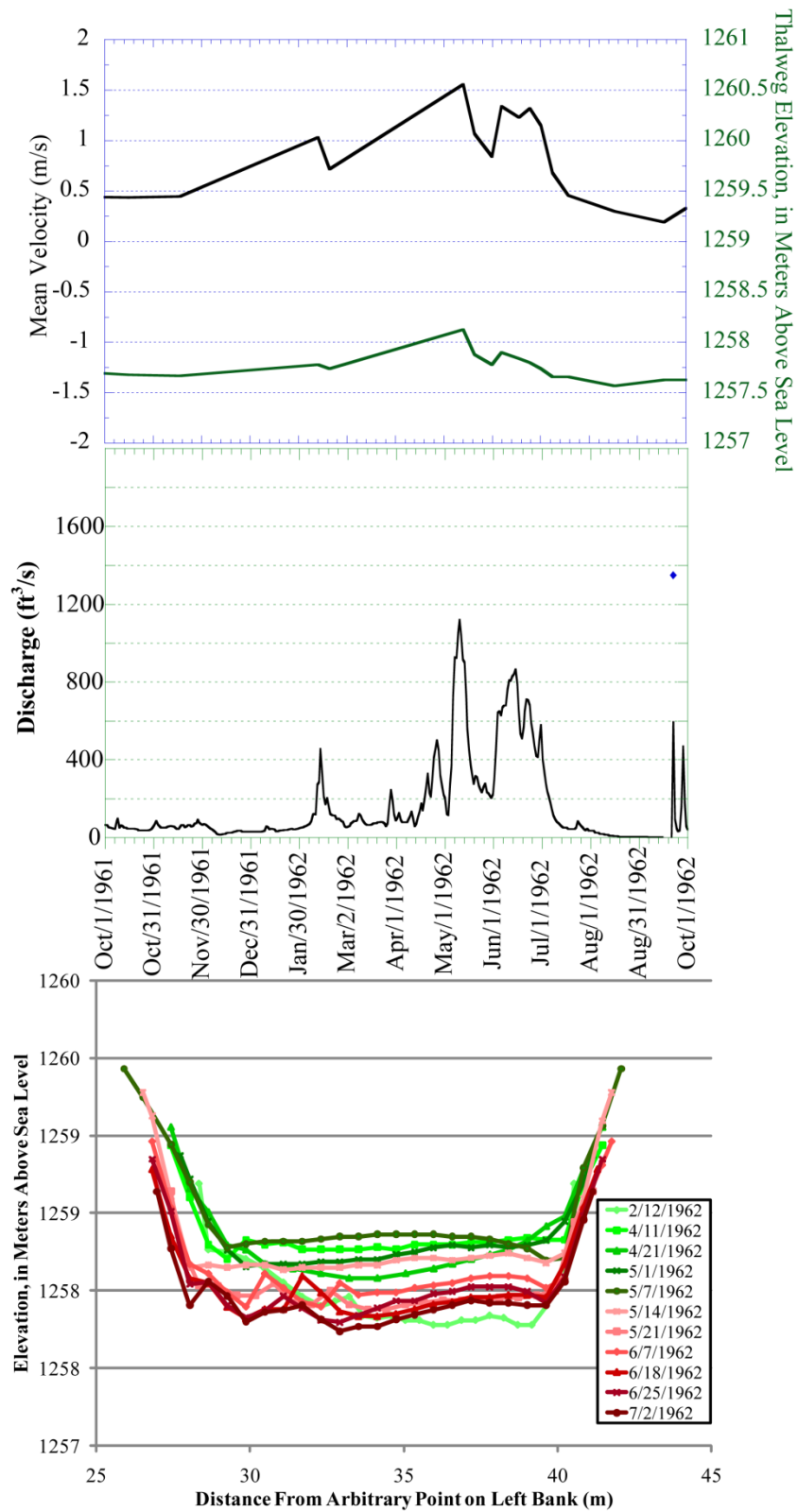


**Figure 35. Cross sections and time series of discharge, MINSBE and velocity during the progress of the snowmelt flood of 1962. Cross sections colored green were measured during the rising limb of the flood hydrograph. Cross sections in red were measured during the falling limb.**

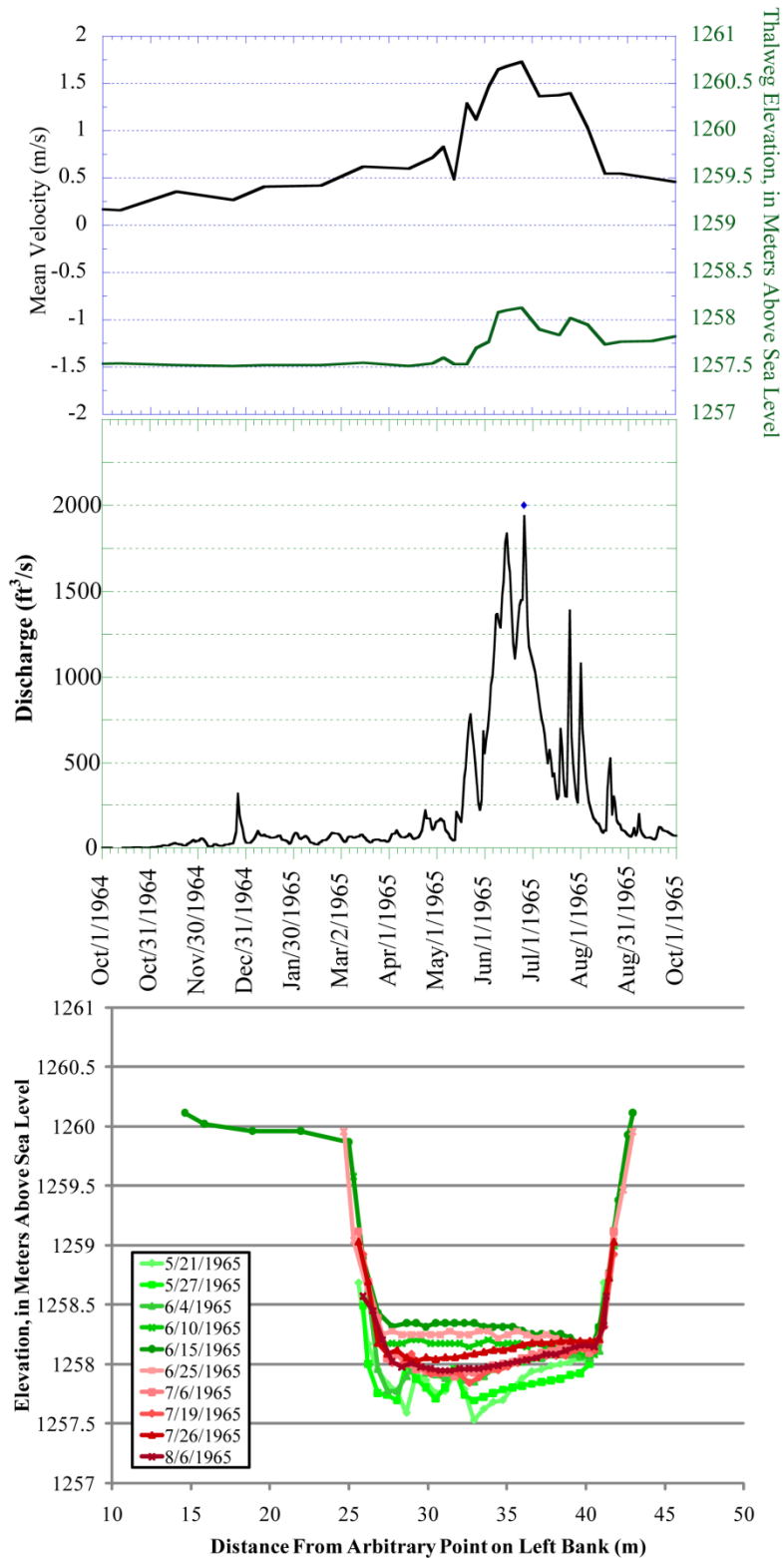


**Figure 36. Cross sections and time series of discharge, MINSBE and velocity during the progress of the snowmelt flood of 1965. Cross sections colored green were measured during the rising limb of the flood hydrograph. Cross sections in red were measured during the falling limb**

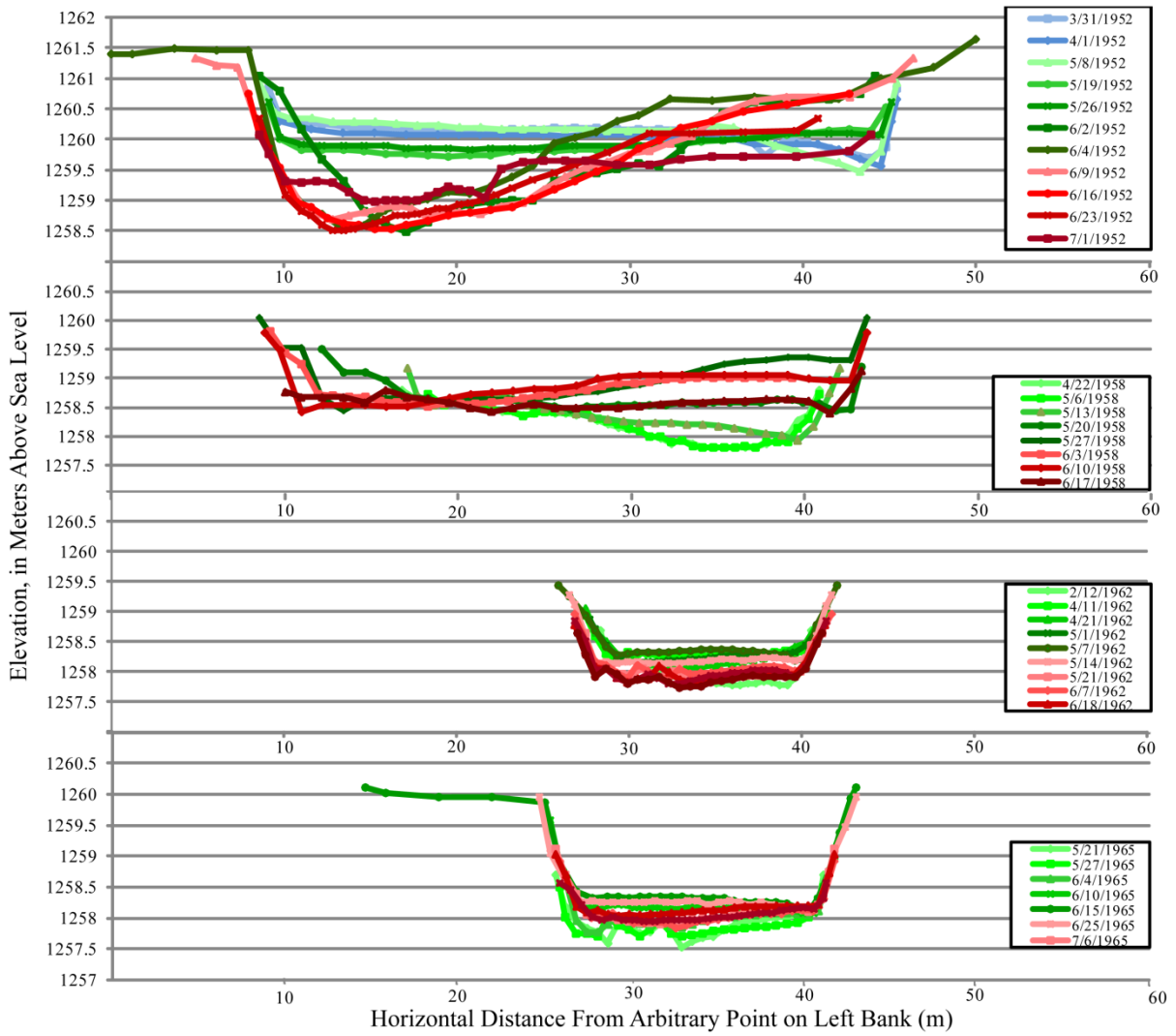


**Figure 37. Cross sections measured during the snowmelt floods of 1952, 1958, 1962, 1965. Cross sections in shades of green were measured during the rising limb of the flood hydrograph. Cross sections in shades of red were measured during the falling limb.**

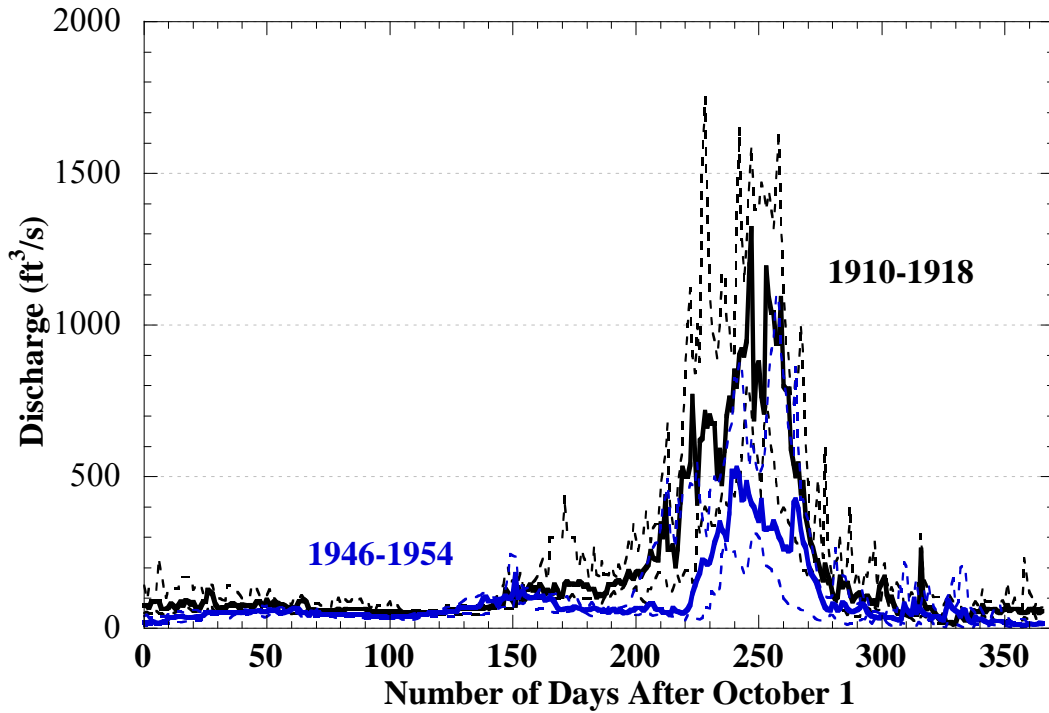


Figure 38. Median annual hydrograph for two time periods. 1910-1918 is shown in blue and 1945-1954 is shown in black. Dotted lines are the lower and upper quartiles for each time period.

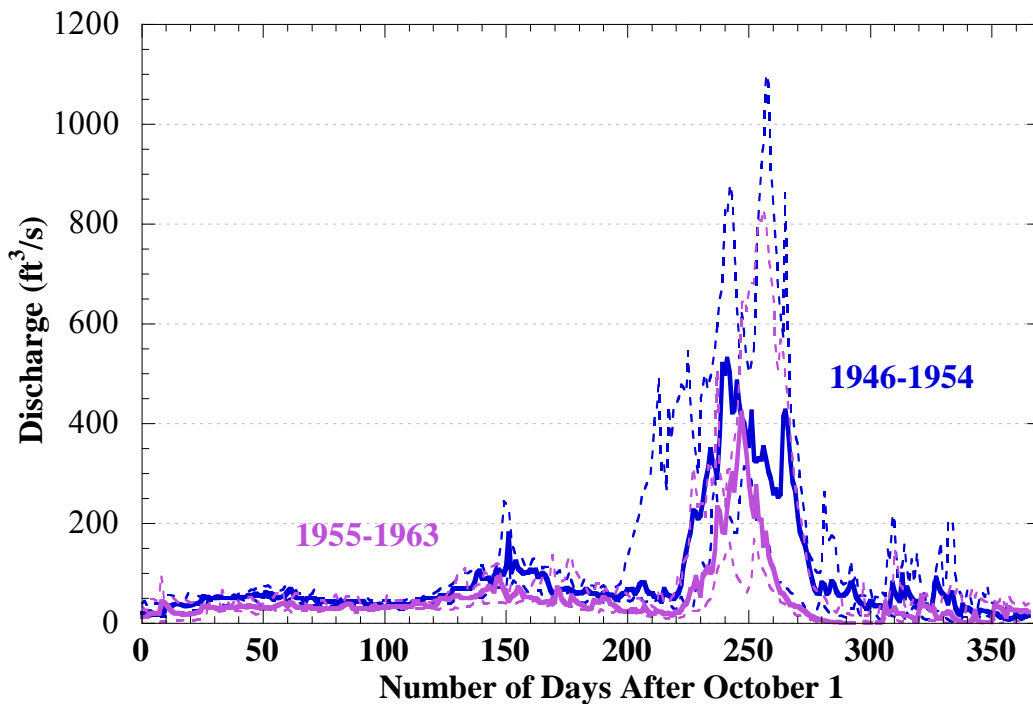


Figure 39. Median annual hydrograph for two time periods. 1946-1954 is shown in blue and 1955-1963 is shown in purple. Dotted lines are the lower and upper quartiles for each time period.